Bub1 overexpression induces aneuploidy and tumor formation through Aurora B kinase hyperactivation

Robin M. Ricke,[1] Karthik B. Jeganathan,[1] and Jan M. van Deursen[1,2]

[1]Department of Pediatric and Adolescent Medicine, [2]Biochemistry and Molecular Biology, Mayo Clinic, Rochester, MN 55905

High expression of the protein kinase Bub1 has been observed in a variety of human tumors and often correlates with poor clinical prognosis, but its molecular and cellular consequences and role in tumorigenesis are unknown. Here, we demonstrate that overexpression of Bub1 in mice leads to near-diploid aneuploidies and tumor formation. We found that chromosome misalignment and lagging are the primary mitotic errors responsible for the observed aneuploidization. High Bub1 levels resulted in aberrant Bub1 kinase activity and hyperactivation of Aurora B kinase. When Aurora B activity is suppressed, pharmacologically or via BubR1 overexpression, chromosome segregation errors caused by Bub1 overexpression are largely corrected. Importantly, Bub1 transgenic mice overexpressing Bub1 developed various kinds of spontaneous tumors and showed accelerated Myc-induced lymphomagenesis. Our results establish that Bub1 has oncogenic properties and suggest that Aurora B is a critical target through which overexpressed Bub1 drives aneuploidization and tumorigenesis.

Introduction

During M phase, replicated chromosomes are evenly distributed into daughter cells. Inaccurate chromosome segregation can result in the loss or gain of whole chromosomes, a status referred to as aneuploidy (Ricke et al., 2008). Aneuploidy is observed in 80–90% of human cancers and associated with poor clinical outcome, but its role in malignant cell transformation remains ambiguous (Holland and Cleveland, 2009; Schvartzman et al., 2010). To ensure faithful chromosome segregation, eukaryotic cells have developed a surveillance system, the mitotic checkpoint, which delays anaphase onset until all kinetochores are properly attached to microtubules emanating from opposite spindle poles (Nezi and Musacchio, 2009). One of the core components of this checkpoint is Bub1 (Roberts et al., 1994; Taylor and McKeon, 1997). In prophase, this serine/threonine protein kinase accumulates at unattached kinetochores where it mediates the recruitment of Mad1–Mad2 dimers (Sharp-Baker and Chen, 2001; Meraldi and Sorger, 2005; Jeganathan et al., 2007). These Mad1–Mad2 dimers produce a diffusible anaphase wait signal consisting of protein complexes of Bub3, BubR1, and Mad2 (Sudakin et al., 2001; Luo et al., 2002; Sironi et al., 2002; Kulukian et al., 2009). These complexes bind to and inhibit Cdc20, the activating subunit of the anaphase-promoting complex/cyclosome (APC/C), an E3 ubiquitin ligase that regulates orderly separation of chromosomes by targeting various cell cycle regulators for degradation by the 26S proteasome at specific mitotic stages (Peters, 2006). Bub1 not only regulates APC/C activity via kinetochore recruitment of Mad1–Mad2, but has also been proposed to inhibit APC/C activity directly through phosphorylation of Cdc20 (Chung and Chen, 2003; Tang et al., 2004a).

In addition to the Mad proteins, several other mitotic proteins are dependent on Bub1 for efficient recruitment to unattached kinetochores, including BubR1, Cenp-E, and Sgo1 (Sharp-Baker and Chen, 2001; Tang et al., 2004b; Morrow et al., 2005; Jeganathan et al., 2007; Perera et al., 2007). BubR1 and Cenp-E both function in microtubule–kinetochore attachment and failure to recruit these proteins at unattached kinetochores is known to cause chromosome missegregation (Wood et al., 1997; Yao et al., 2000; Lampson and Kapoor, 2005; Malureanu et al., 2009). Sgo1, on the other hand, acts to maintain centromeric cohesion of duplicated chromosomes until bi-orientation has been accomplished (Tang et al., 2004b; Boyarchuk et al., 2007; Kawashima et al., 2010). The current model is that Bub1

Correspondence to Jan van Deursen: vandeursen.jan@mayo.edu

Abbreviations used in this paper: CAGGS, CMV early enhancer/chicken β-actin; CPC, chromosome passenger complex; HA, hemagglutinin; MEF, mouse embryonic fibroblast; PMSCS, premature sister chromatid separation.

The Rockefeller University Press $30.00
J. Cell Biol. Vol. 193 No. 6 1049–1064
www.jcb.org/cgi/doi/10.1083/jcb.201012035

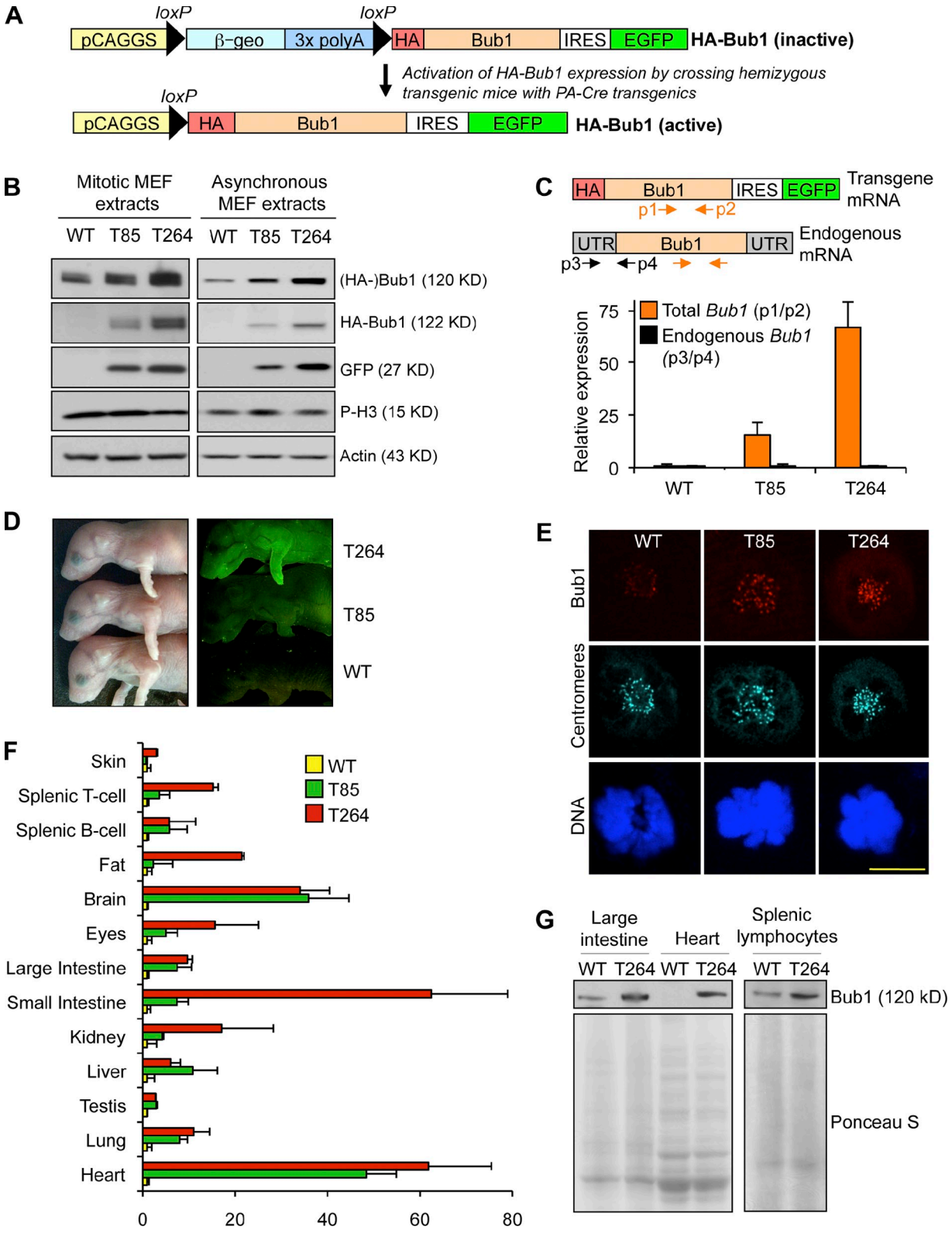

Figure 1. ***Bub1* transgenic mice overexpress Bub1 protein in a wide variety of tissues and cell types.** (A) Overview of the approach used to generate *Bub1* transgenic mouse strains. (Top) Transgenic mice were generated in which the *HA-Bub1* and *EGFP* transgenes are inactive due to the presence of a floxed β-geo "STOP" cassette (consisting of β-galactosidase-neomycin fusion gene and three tandemly arranged polyadenylation sites) immediately downstream of the CAGGS promoter. We bred these transgenics to protamine-Cre transgenic mice (O'Gorman et al., 1997) to excise the STOP cassette in the male germline. (Bottom) Breeding of double-transgenic males to wild-type females, yielded offspring in which the CAGGS promoter was juxtaposed with the *HA-Bub1* and *EGFP* coding regions in all cells. IRES, internal ribosomal entry site; PA, protamine. (B) Immunoblot analysis of mitotic and asynchronous lysates from transgenic and wild-type primary MEFs. Blots were probed for endogenous Bub1 (Bub1), exogenous HA-Bub1 (HA), and GFP (GFP). Actin and pH3 were used as loading controls. (C) QRT-PCR for *Bub1* transcripts in cycling MEFs of the indicated genotypes. Orange and black arrows mark primer

phosphorylates threonine 121 of histone H2A at inner centromeres (Kawashima et al., 2010), thereby creating a local docking site for Sgo1. In turn, Sgo1 then allows for recruitment of PP2A to inner centromeres, a protein phosphatase that retains cohesin at centromeres by counteracting Plk1 kinase activity (Tang et al., 2006).

Mutations in Bub1 and other mitotic checkpoint genes are relatively rare in human cancers (Cahill et al., 1998, 1999; Gemma et al., 2000; Jaffrey et al., 2000; Sato et al., 2000). On the other hand, deregulation of mitotic checkpoint gene expression seems to occur at much higher incidence. For instance, reduced Bub1 expression has been detected in a subset of lung, colon, and pancreatic tumors (Shichiri et al., 2002; Hempen et al., 2003). Mouse models mimicking these reductions are prone to aneuploidy and cancer, indicating that Bub1 insufficiency can increase cancer risk (Jeganathan et al., 2007; Baker et al., 2009; Schliekelman et al., 2009). A far more common event in human tumors may be up-regulation of mitotic factors and several studies have found high Bub1 levels in subsets of breast and gastric cancers, and lymphomas (Alizadeh et al., 2000; Shigeishi et al., 2001; van't Veer et al., 2002; Grabsch et al., 2003, 2004; Basso et al., 2005). Furthermore, independent studies of diverse tumor types have identified Bub1 as a gene whose up-regulation correlates with poor clinical prognosis (Sotiriou et al., 2003; Glinsky et al., 2005; Nakagawa et al., 2008). Based on these observations, it is tempting to speculate that there might be a causal relationship between up-regulation of Bub1 and tumorigenesis. However, because Bub1 expression is relatively high in proliferating cells compared with quiescent or differentiated cells (Perera et al., 2007), increased Bub1 levels may simply represent an increase in the mitotic index of the tumors compared with neighboring tissue. Thus, even though elevated Bub1 gene expression seems to be a useful prognostic marker for systemic progression of certain types of tumors, whether high Bub1 levels can drive neoplastic transformation and/or tumor aggressiveness has not yet been established. In addition, the molecular and physiological consequences of Bub1 up-regulation are not known.

To address these key questions, we generated transgenic mouse strains that overexpress Bub1 in a wide variety of tissues. Here, we demonstrate that Bub1 overexpression causes chromosome misalignment and chromosome lagging resulting in near-diploid aneuploidies. We further show that high Bub1 levels lead to aberrant phosphorylation of H2A and hyperactivation of Aurora B kinase. We find that high-fidelity chromosome segregation in Bub1 transgenic cells can be restored by inhibition of Aurora B, implying that Aurora B is the critical target through which overexpressed Bub1 drives aneuploidization. Furthermore, we show that Bub1 overexpression drives spontaneous tumorigenesis and accelerates the development of Eμ-Myc–induced lymphomas, firmly establishing that Bub1 has oncogenic properties.

Results

Generation of Bub1 transgenic mice

To test whether Bub1 has oncogenic properties in vivo, we generated transgenic mice that express the mouse *Bub1* coding sequence under control of the CMV early enhancer/chicken β-actin (CAGGS) promoter (Fig. 1 A). To facilitate transgene detection, the *Bub1* start codon was replaced by a double hemagglutinin (HA) tag sequence. EGFP was coexpressed from an internal ribosomal entry site (IRES) to serve as a reporter for HA-Bub1 expression. Two independent *HA-Bub1* transgenic mouse lines were obtained. Hereafter we will refer to these lines as *Bub1*^{T85} (T85) and *Bub1*^{T264} (T264). Mice of both transgenic lines were overtly normal and obtained at expected Mendelian frequency (unpublished data). The mouse genetic background was mixed 129SV/E X C57BL/6. Western blot analysis of mouse embryonic fibroblasts (MEFs), testis, and ovary from pure C57BL/6 and 129 wild-type mice confirmed that genetic background itself does not vary Bub1 levels (Fig. S1, A and B). Furthermore, there were no differences in karyotypic stability between MEFs derived from pure C57BL/6 and 129 mice (Fig. S1 C).

To assess the level of Bub1 overexpression in *Bub1*^{T85} and *Bub1*^{T264} mice, we first performed Western blot analysis on MEFs derived from these mice. As shown in Fig. 1 B, mitotic extracts from *Bub1*^{T85} and *Bub1*^{T264} MEFs had substantially higher Bub1 protein levels than those from wild-type MEFs. *Bub1*^{T264} MEFs showed the highest levels of Bub1 overexpression and are estimated to contain six- to sevenfold more Bub1 than wild-type MEFs (Fig. S1 D). Very similar results were obtained with cell extracts from asynchronous MEF cultures (Fig. 1 B). *Bub1* expression levels were further examined using quantitative (q)RT-PCR. Total (endogenous and transgenic) *Bub1* transcript levels were 15- and 67-fold increased compared with wild type in *Bub1*^{T85} and *Bub1*^{T264} MEFs, respectively (Fig. 1 C). The difference in transgene expression between the *Bub1*^{T85} and *Bub1*^{T264} MEFs correlated with EGFP levels in newborn pups (Fig. 1 D). Immunolabeling experiments with polyclonal antibodies revealed that the level of kinetochore-associated Bub1 is substantially higher in transgenic MEFs than in wild-type MEFs, with *Bub1*^{T264} MEFs showing the most profound increase (Fig. 1 E). Immunostaining for HA confirmed that HA-Bub1 is properly targeted to kinetochores at mitosis onset (not depicted).

The CAGGS promoter cassette that we used is known to be ubiquitously active in mice (Novak et al., 2000). To investigate the tissue distribution of transgene expression in *Bub1*^{T85}

positions for analysis of total (endogenous and exogenous, p1/p2) and endogenous *Bub1* (p3/p4), respectively. Data shown are the mean ± SEM (n = 3 independent cell lines, in triplicate). Values were normalized to *TBP*. (D) EGFP fluorescence from 1-d-old pups of the indicated genotypes. (E) Representative images of wild-type, *Bub1*^{T85}, and *Bub1*^{T264} MEFs in prometaphase coimmunostained with anti-Bub1 and anti-centromere antibodies. DNA was visualized with Hoechst. Bar, 10 μm. (F) Total *Bub1* transcripts in various tissues and cell types from mice of the indicated genotypes (primer pair p1/p2 was used in this qRT-PCR analysis). Data shown are the mean ± SEM (n = 3 mice per genotype, in triplicate). Values were normalized to *TBP* except bone marrow, which was normalized to GAPDH. (G) Western blot analysis of extracts of the indicated tissues and cell types for Bub1. Ponceau S served as a loading control.

Table I. **Overexpression of Bub1 in MEFs induces progressive near-diploid aneuploidy**

MEF genotype (*n*)	Mitotic figures inspected	Aneuploid figures (SD)	Karyotypes with indicated chromosome number							Mitotic figures with PMSCS (SD)
			37	38	39	40	41	42	43	
		%								%
WT (3)	150	11 (1)	2	1	5	133	7	2		1 (1)
Bub1^{T85} (3)	150	21 (1)	2	1	9	118	15	5		8 (0)
WT (3)	150	11 (1)			5	133	8	3	1	3 (1)
Bub1^{T264} (3)	150	25 (1)	1	3	22	113	9	2		12 (1)

Empty spaces mean that there were no karyotypes with the indicated chromosome number. Karyotyping was performed at passage 5.

and *Bub1*^{T264} mice, we collected a variety of tissues from 6–8-wk-old mice and extracted RNA for qRT-PCR analysis. As shown in Fig. 1 F, most tissues from transgenic mice have substantially higher *Bub1* transcript levels than corresponding wild-type tissues, although the actual fold increase varied per tissue. Furthermore, although *Bub1*^{T264} transgenic mice expressed higher transcript levels than *Bub1*^{T85} mice in several tissues, including fat, eye, and small intestine, other tissues, like brain, lung, and large intestine, showed quite similar transcript levels. A complementary analysis of the relative expression levels of *Bub1* per organ is presented in Fig. S1 E. Furthermore, Western blot analysis of protein extracts from select tissues of wild-type and *Bub1*^{T264} mice yielded results that were consistent with those obtained by qRT-PCR analysis (Fig. 1 G). Taken together, these data indicate that our transgenic mouse lines widely overexpress *Bub1*.

Bub1 overexpression causes chromosome missegregation and near diploid aneuploidy

To determine if Bub1 overexpression affects karyotype stability, we performed chromosome counts on metaphase spreads of passage 5 (P5) wild-type, *Bub1*^{T85}, and *Bub1*^{T264} MEFs. Aneuploidy was observed in 11% of wild-type spreads (Table I). In contrast, aneuploidy rates were substantially higher in both *Bub1*^{T85} and *Bub1*^{T264} MEFs, with 21% and 25% of cells showing aneuploidy, respectively (Table I). Moreover, we observed premature sister chromatid separation (PMSCS) in 8 and 12% of *Bub1*^{T85} and *Bub1*^{T264} spreads, respectively, but only in 1–3% of wild-type MEFs (Table I). Like wild-type MEFs, metaphase spreads of *Bub1* transgenic MEFs had no overtly detectable structural chromosome abnormalities, such as chromosome breaks, gaps, and fusions (unpublished data).

Chromosome counts on hepatic lymphocytes revealed that *Bub1*^{T85} and *Bub1*^{T264} mice already had acquired substantial aneuploidy at birth (Table II). An even higher rate of aneuploidy was observed in splenic lymphocytes of 6-wk-old *Bub1*^{T85} and *Bub1*^{T264} mice, with 31 and 30% of spreads showing aneuploidy, respectively. However, no further increases were observed at 5 mo of age. PMSCS rates were very low in both *Bub1*^{T85} and *Bub1*^{T264} lymphocytes (Table II), indicating that Bub1 overexpression does not aberrantly affect chromosome cohesin in this cell type. Furthermore, there was no evidence for overt structural chromosome instability in *Bub1* transgenic lymphocytes (unpublished data).

To assess the mitotic defects that promote aneuploidy due to increased Bub1, we monitored chromosome segregation in primary transgenic MEFs through an unperturbed mitosis by live-cell imaging (van Ree et al., 2010). MEFs were infected with a lentivirus encoding mRFP-H2B to permit visualization of chromosomes by fluorescence microscopy. The common defect in both clones of Bub1 transgenic MEFs was chromosome lagging (Fig. 2, A and B), a defect believed to be caused by the aberrant attachment of one kinetochore to both spindle poles, referred to as merotelic attachment. Recent studies indicate that such attachments can result from spindle defects caused by centrosome

Table II. **Increasing aneuploidy in lymphocytes from Bub1 transgenic mice**

Mouse genotype	Age (*n*)	Mitotic figures inspected	Aneuploid figures (SD)	Karyotypes with indicated chromosome number								Mitotic figures with PMSCS (SD)
				36	37	38	39	40	41	42	43	
			%									%
WT	1 d (3)	150	1 (1)			1		148			1	1 (1)
WT	6 wk (3)	150	2 (2)				2	147	1			1 (2)
WT	5 mo (3)	150	4 (0)			1	2	144	3			1 (1)
Bub1^{T85}	1 d (3)	150	21 (3)	3	3	5	14	119	5	1		3 (1)
Bub1^{T85}	6 wk (3)	150	31 (2)		1	8	17	104	13	4	3	3 (1)
Bub1^{T85}	5 mo (3)	150	35 (6)	4	4	11	23	97	8	3		1 (2)
Bub1^{T264}	1 d (3)	150	15 (2)	2	1	4	8	127	7	1		0 (0)
Bub1^{T264}	6 wk (3)	150	30 (3)	4	1	6	15	105	14	5		3 (1)
Bub1^{T264}	5 mo (3)	150	28 (2)	2	1	8	16	108	12	3		6 (3)

Empty spaces mean that there were no karyotypes with the indicated chromosome number.

A

MEF genotype (n)	Mitotic cells inspected	Cells with segregation defects	Metaphases with misaligned chromosomes	Anaphases with lagging chromosomes	Anaphases with chromosomes bridges
		% (SEM)	% (SEM)	% (SEM)	% (SEM)
WT (5)	100	14 (2)	0 (0)	11 (1)	3 (1)
Bub1^{T85} (3)	63	30 (2)	0 (0)	22 (5)	5 (5)
Bub1^{T264} (3)	62	33 (2)	12 (2)	20 (3)	6 (6)

B

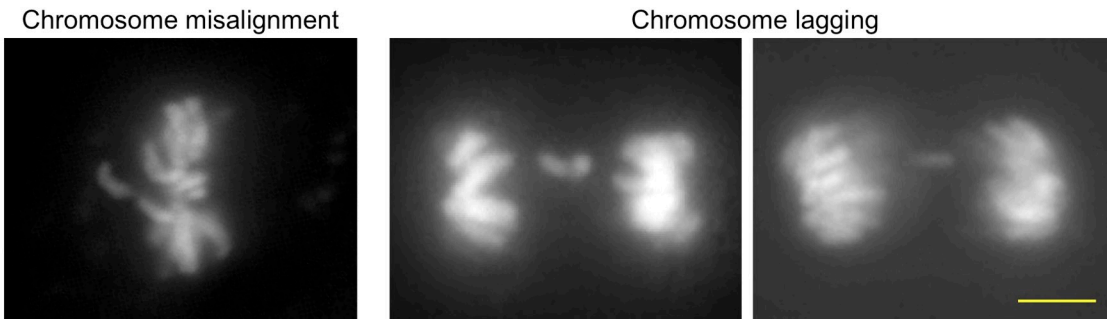

Figure 2. **Bub1 overexpression causes chromosome missegregation.** (A) Live-cell imaging analysis of chromosome segregation defects in primary MEFs with indicated genotypes. (B) Representative images of cells with indicated chromosome missegregation events. Bar, 10 µm.

amplification (Ganem et al., 2009; Silkworth et al., 2009). However, this mechanism is unlikely to underlie merotely in *Bub1* transgenic MEFs because *Bub1*^{T264} MEFs showed no evidence of supernumerary centrosomes when immunostained for centrin 2 (Fig. S2 A).

To determine whether chromosome segregation initiated in the presence of unaligned chromosomes would be corrected with more time in mitosis, we extended metaphase with the addition of MG132. Under these conditions, *Bub1*^{T264} MEFs were able to obtain full alignment with kinetics similar to wild-type MEFs (Fig. S2 B), raising the possibility that Bub1 overexpression drives misalignment by accelerating time to anaphase onset. To explore this, we followed mRFP-H2B–positive transgenic and wild-type MEFs through mitosis and calculated the duration of each mitotic stage. We found that mitotic timing of *Bub1*^{T264} MEFs was comparable to wild-type and *Bub1*^{T85} MEFs (Fig. S2 C). Alternatively, because Bub1 is a key component of the mitotic checkpoint, the chromosome segregation defects observed in *Bub1* transgenic MEFs might be due to mitotic checkpoint weakening. To assay for this, we challenged primary MEFs with two different spindle poisons, nocodazole or taxol, in cells that were infected with lentivirus encoding mRFP-H2B (van Ree et al., 2010). Importantly, *Bub1*^{T85} and *Bub1*^{T264} MEFs were equally able to maintain an arrest in response to nocodazole or taxol, similar to wild type (Fig. S2, D and E). Consistent with this, we found that kinetochore localization of core mitotic checkpoint proteins that accumulate at unattached kinetochores, including BubR1, Cdc20, Mad2, and Cenp-E, was normal in *Bub1* transgenic MEFs (Fig. S2 F, and unpublished data). Together, these data suggested that Bub1 overexpression does not interfere with mitotic checkpoint signaling or kinetochore assembly, and imply that the chromosome segregation defects observed in *Bub1* transgenic MEFs are invisible from either checkpoint detection or resolution, and not due to rapid anaphase onset.

Bub1 overexpression leads to aberrant substrate phosphorylation

Selective loss of Bub1 kinase activity in HeLa cells has been shown to promote chromosome misalignment (Meraldi and Sorger, 2005; Klebig et al., 2009), suggesting that Bub1's catalytic activity plays a role in microtubule–kinetochore attachment. To test whether Bub1 overexpression leads to aberrant catalytic activity, we made use of the recent discovery that Bub1 kinase phosphorylates histone H2A at threonine 121 in humans (Kawashima et al., 2010), a site that is conserved in mouse. In wild-type MEFs, pT121-H2A antibody stained kinetochores in prophase and prometaphase (Fig. 3 A). This staining remained detectable in metaphase but at reduced intensity, and was completely abolished when cells progressed to anaphase. In prophase, H2A phosphorylation at centromeres was much higher in *Bub1*^{T264} MEFs than in wild-type MEFs. Furthermore, in prometaphase, H2A phosphorylation was not only much higher at centromeres, but now also occurred along chromosome arms (Fig. 3 A). In metaphase, H2A phosphorylation persisted at both locations, but was less abundant than in prometaphase. In anaphase, no H2A phosphorylation was detectable, similar to wild-type MEFs (Fig. 3 A). The pattern of H2A phosphorylation in *Bub1*^{T85} MEFs mirrored that of *Bub1*^{T264} MEFs, although the amount of phosphorylation at centromeres and chromosome arms was typically lower than in *Bub1*^{T264} MEFs (Fig. 3, B and C), suggesting that Bub1 overexpression correlates with aberrant Bub1 catalytic activity. Consistently, by Western blotting we observed

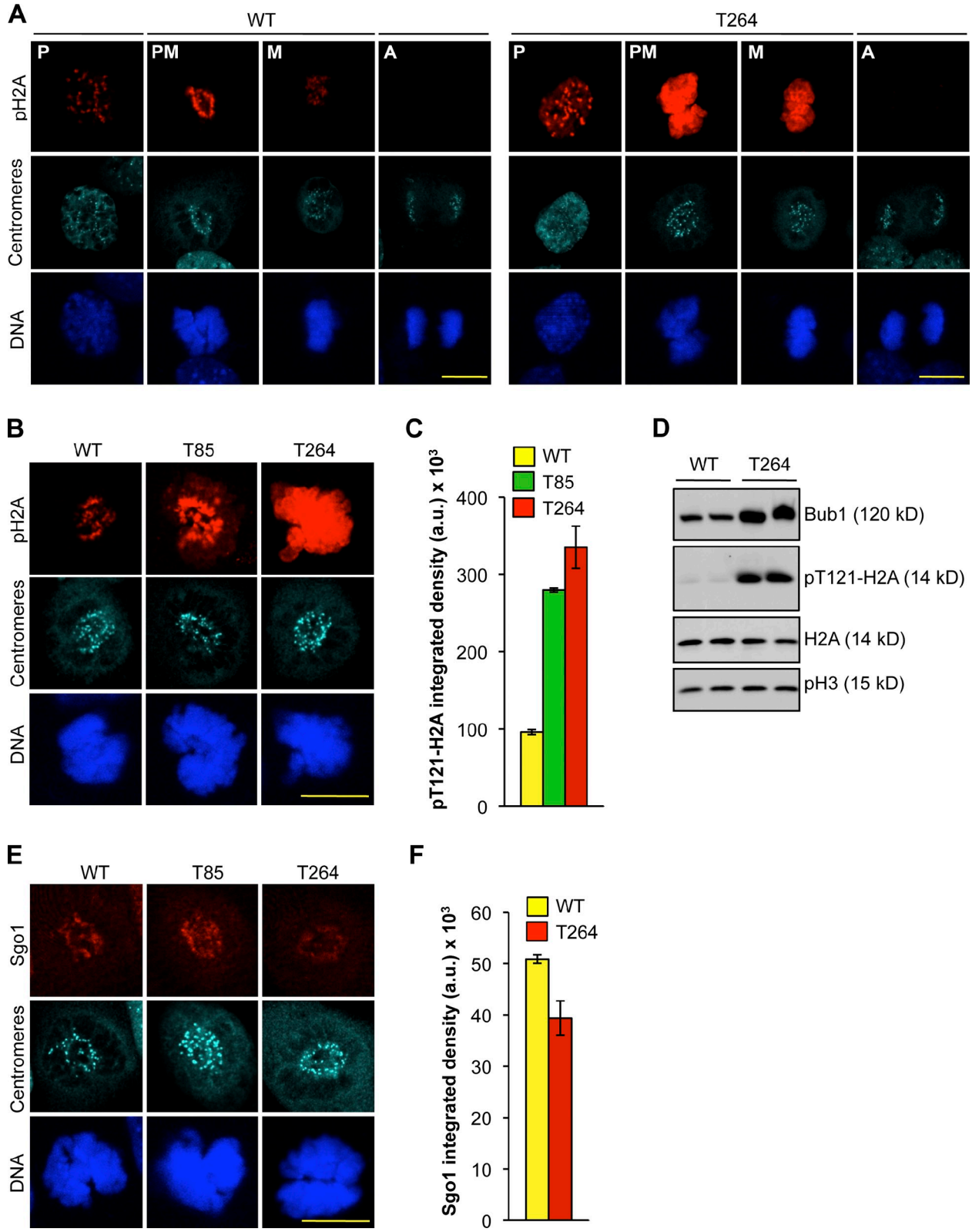

Figure 3. **Bub1 overexpression results in aberrant Bub1 substrate phosphorylation.** (A) Representative images of wild-type and *Bub1*^{T264} MEFs at the indicated stages of mitosis that were immunostained for pT121-H2A and centromeres. DNA was visualized with Hoechst. Bar, 10 µm. (B) Representative images of wild-type, *Bub1*^{T85}, and *Bub1*^{T264} prometaphases that were immunostained for pT121-H2A and centromeres. DNA was visualized with Hoechst. Bar, 10 µm. (C) Quantification of pT121-H2A signal of images from B. Data shown are the average of three independent lines and error bars represent SEM. (D) Protein extracts from cycling MEFs of the indicated genotype were blotted and probed for Bub1, pT121-H2A, H2A, and pS10-H3. (E) Representative images of wild-type, *Bub1*^{T85}, and *Bub1*^{T264} prometaphases that were immunostained for centromeres and Sgo1. DNA was visualized with Hoechst. Bar, 10 µm. (F) Quantification of Sgo1 signal of images from E. Data are the average of three independent lines and error bars represent SEM.

more phosphorylated H2A in an asynchronous population of cells in *Bub1*^{T264} cells compared with wild type (Fig. 3 D).

Kawashima et al. (2010) reported H2A phosphorylation of the entire chromosome by ectopically expressed Bub1 kinase domain fused to H2B results in relocation of centromere-associated Sgo1 to chromosome arms. However, we found that Sgo1 was properly localized to the centromeric regions of *Bub1*^{T85} MEFs in prometaphase (Fig. 3 E), when H2A phosphorylation was high along chromosome arms (Fig. 3, B and C). Although *Bub1*^{T264} MEFs had slightly reduced Sgo1 levels at inner centromeric regions (Fig. 3, E and F), there was no detectable increase in Sgo1 staining along chromosome arms in any *Bub1*^{T264} cell analyzed. An inverse relationship between Bub1 and Sgo1 abundance at kinetochores has previously been reported (Pouwels et al., 2007; Daum et al., 2009), although the exact nature of the relationship is currently unclear.

Overexpression of Bub1 results in Aurora B hyperactivation

Earlier in vitro studies using *Xenopus* oocyte extracts have suggested that Bub1 not only phosphorylates H2A but also INCENP, although the precise residues targeted by Bub1 remain to be identified (Boyarchuk et al., 2007). INCENP is a component of the chromosome passenger complex (CPC), which further consists of Aurora B, Borealin, Survivin, and TD-60 (Carmena et al., 2009). It has been proposed that INCENP binding to Aurora B activates basal Aurora B kinase activity, and that phosphorylation of INCENP by Bub1 induces a feedback loop of additional activation (Kang et al., 2001; Bishop and Schumacher, 2002; Honda et al., 2003; Sessa et al., 2005; Boyarchuk et al., 2007). These findings prompted the hypothesis that Bub1 hyperactivity in transgenic MEFs might deregulate the proper control of Aurora B kinase activity, an idea that was reinforced by reports demonstrating that Aurora B contributes to the regulation of kinetochore–microtubule attachment (Cimini et al., 2006). Aurora B does this, at least in part, through regulating the microtubule-depolymerizing activity of MCAK and the microtubule-capturing activity of Ndc80/Hec1 (Andrews et al., 2004; Cheeseman et al., 2006; Knowlton et al., 2006).

To explore the role of Aurora B in chromosome missegregation induced by Bub1 overexpression, we first asked whether Aurora B kinase activity was aberrantly affected in Bub1 transgenic MEFs. As a functional assessment of Aurora B activity, we measured the degree of Cenp-A and Knl1 phosphorylation using immunofluorescence microscopy (Zeitlin et al., 2001; Welburn et al., 2010). In prophase, phosphorylated Cenp-A (pCenpA) and phosphorylated Knl1 (pKnl1) staining were both significantly higher in *Bub1*^{T264} MEFs than in wild-type MEFs (Fig. 4, A–D), indicating that Aurora B might indeed become hyperactive upon Bub1 overexpression.

To begin to address how Bub1 may alter Aurora B activity, we monitored Aurora B localization. Targeting of Aurora B to inner centromeric regions of mitotic chromosomes was unperturbed in *Bub1*^{T264} MEFs (Fig. S3 A), indicating that *Bub1* overexpression does not alter the spatial regulation of Aurora B. Western blot analysis of mitotic extracts of wild-type and *Bub1*^{T264} MEFs revealed that Bub1-overexpressing cells have normal amounts of T232-phosphorylated Aurora B (Fig. S3 B). Furthermore, mitotic *Bub1*^{T264} MEFs had normal amounts of pT232-Aurora B at inner centromeric regions (Fig. S3 C). However, we note that auto-activation of Aurora B through phosphorylation represents an incomplete assessment of total catalytic activity. For example, in vitro Aurora B activity is not proportional to phosphorylated Aurora B when INCENP is added (Bishop and Schumacher, 2002; Sessa et al., 2005). Moreover, the amount of pT232-Aurora B in vivo was unaffected by haspin siRNA although Aurora B is delocalized and results in less centromeric MCAK (Wang et al., 2010). In addition, Ndc80/Hec1 has recently been shown to be de-phosphorylated even in the presence of phosphorylated Aurora B (DeLuca et al., 2011).

To determine how Bub1 may affect Aurora B activity, we sought to determine whether Bub1 and Aurora B were present in a complex. Using coimmunoprecipitation, we found that a subset of endogenous Bub1 and Aurora B exists in a complex in wild-type MEFs and that Bub1 overexpression considerably increases the amount of Aurora B that is bound to Bub1 (Fig. 4 E). Importantly, we were able to confirm that a subset of Bub1 and Aurora B forms a complex in mitotic Hela cells (Fig. 4 F).

Bub1-induced Aurora B hyperactivity drives chromosome missegregation and aneuploidy

To test whether Aurora B hyperactivity might drive, at least in part, chromosome missegregation in Bub1 overexpression cells, we sought to reduce Aurora B kinase activity in *Bub1*^{T85} and *Bub1*^{T264} MEFs with small amounts of the Aurora kinase inhibitor ZM447439 (Ditchfield et al., 2003) and then monitor the accuracy of chromosome segregation by live-cell imaging. At 1 µM ZM447439, cells fail to divide (Ditchfield et al., 2003). Titration experiments revealed that wild-type MEFs experience mild chromosome missegregation at 2.5 nM ZM447439, indicating that Aurora B function is only partially inhibited at this concentration (Fig. 5 A, and unpublished data). Importantly, Bub1 kinase activity was unaffected by this degree of Aurora B inhibition (Fig. S4 A). Remarkably, at 2.5 nM ZM447439, chromosome lagging decreased from 22% to 1% in *Bub1*^{T85} MEFs and from 20% to 1% in *Bub1*^{T264} MEFs (Fig. 5 A). Furthermore, chromosome misalignment in *Bub1*^{T264} MEFs decreased from 12% to 1% (Fig. 5 A). We would like to point out that 15% of MEFs failed to complete mitosis in the presence of 2.5 nM ZM447439, independent of genotype (not depicted). To confirm this effect was due to Aurora B, we undertook a genetic approach of suppressing Aurora B activity by constitutively overexpressing BubR1 (Lampson and Kapoor, 2005). High levels of BubR1 did not reduce Bub1 levels or activity (Fig. S4, B–D). Importantly, misaligned and lagging chromosomes were suppressed when BubR1 is overexpressed in *Bub1*^{T264} cells compared with *Bub1*^{T264} alone (Fig. 5 A). Similarly, lagging chromosomes were suppressed in *Bub1*^{T85} cells co-overexpressing BubR1 (Fig. 5 A).

The corrective effect of BubR1 and treatment with low-dose ZM447439 was further illustrated by counts of chromosome spreads. As shown in Fig. 5 B, high levels of BubR1 restored aneuploidy rates in both *Bub1*^{T85} and *Bub1*^{T264} MEFs to

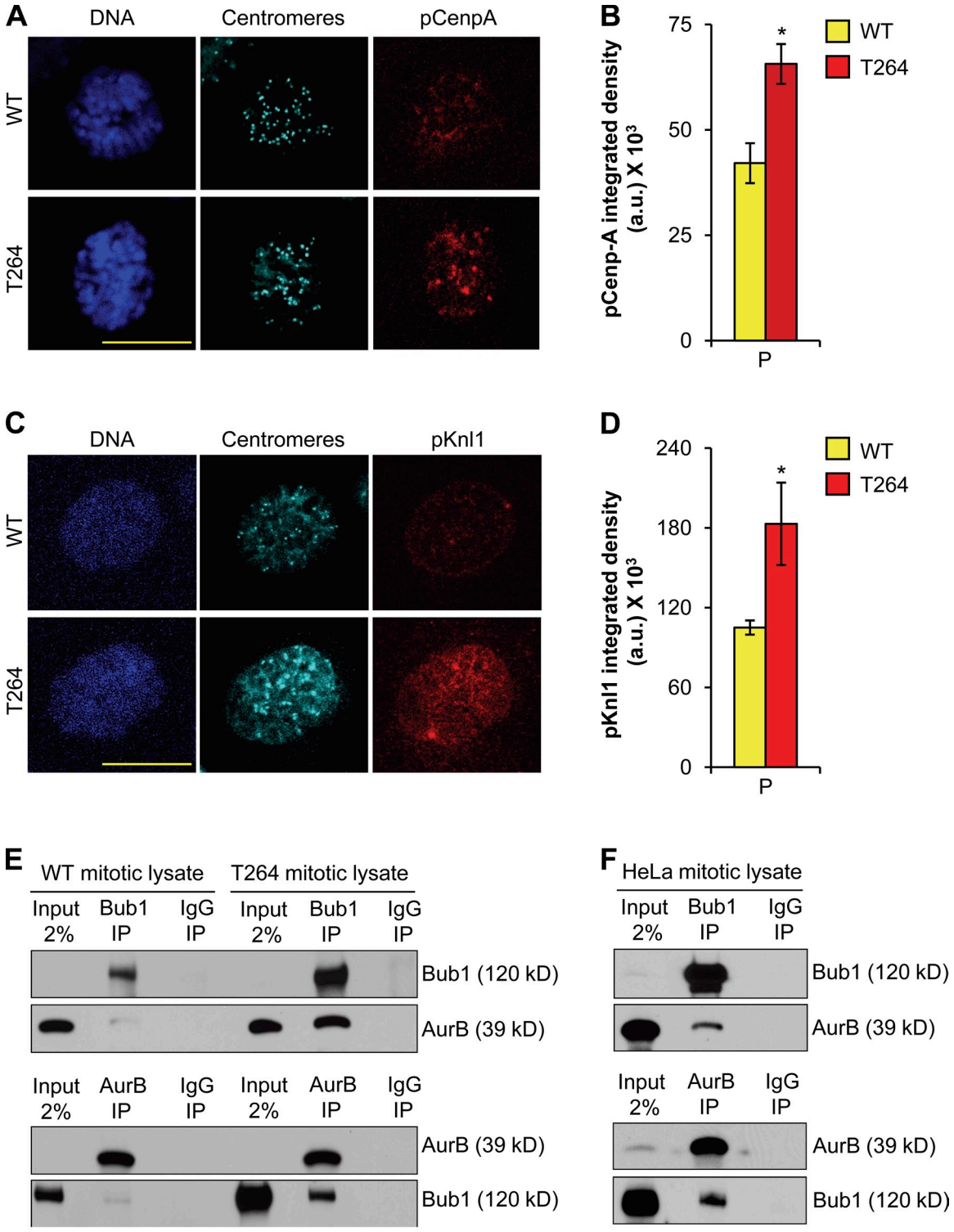

Figure 4. **Aurora B activity is increased in Bub1-overexpressing cells.** (A) Representative images of wild-type and *Bub1*^{T264} prophase cells immunostained for pCenp-A and centromeres. DNA was visualized with Hoechst. Bar, 10 µm. (B) Quantification of the pCenp-A signal using ImageJ software. Error bars represent SEM. *, $P < 0.05$ vs. wild type (unpaired *t* test). (C) Representative images of wild-type and *Bub1*^{T264} prophase cells immunostained for pKnl1 and centromeres. DNA was visualized with Hoechst. Bar, 10 µm. (D) Quantification of the pKnl1 signal using ImageJ software. Error bars represent SEM. *, $P < 0.05$ vs. wild type (unpaired *t* test). (E) Mitotic extracts of wild-type and *Bub1*^{T264} cells subjected to immunoprecipitation with Bub1, Aurora B, or IgG antibodies and analyzed by Western blotting as indicated. (F) Mitotic extracts prepared from taxol-treated HeLa cells subjected to immunoprecipitation with Bub1, Aurora B, or IgG antibodies and analyzed by Western blotting as noted.

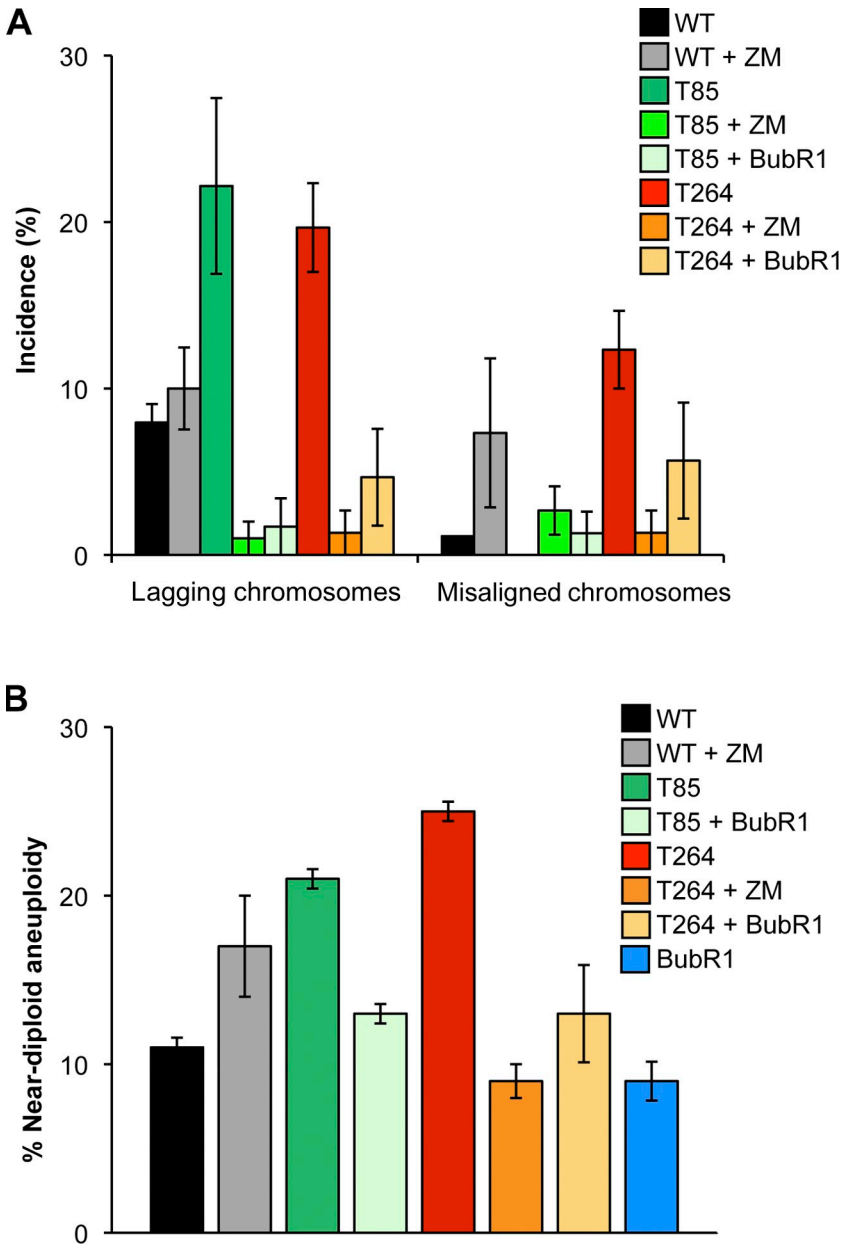

Figure 5. **Aurora B hyperactivation in Bub1-overexpressing cells drives chromosome missegregation and aneuploidization.** (A) Chromosome segregation analysis after treatment with 2.5 nM ZM447439 or constitutive co-overexpression of BubR1. The average of three independent primary MEFs is shown. Error bars represent SEM. (B) Chromosome counts on metaphase spreads of P5 wild-type, *Bub1*^{T85}, and *Bub1*^{T264} MEFs after treatment with 2.5 nM ZM447439 or constitutive co-overexpression of BubR1. The average of three independent lines is shown and error bars represent SEM.

near wild-type levels. To further validate this idea, we determined whether ZM447439 treatment could suppress near-diploid aneuploidy. To do so, we cultured wild-type and *Bub1*^{T264} MEFs from passage P0 to P5 in the presence of 2.5 nM ZM447439. Treatment of *Bub1*^{T264} MEFs with ZM447439 suppressed near-diploid aneuploidy to 9%, whereas aneuploidy in wild-type MEFs increased to 17% (Fig. 5 B). The observation of 17% aneuploidy (but not tetraploidy) in wild-type cells treated with 2.5 nM ZM447439 further confirms partial deregulation of Aurora B activity with this concentration of inhibitor. Finally, immunostaining of *Bub1*^{T264} cells for pKln1 revealed that ZM447439 treatment and BubR1 overexpression each had a substantial corrective effect on aberrant substrate phosphorylation by Aurora B (Fig. S4, E and F; and unpublished data). Collectively, these data suggest that *Bub1* overexpression promotes hyperactivity of Aurora B, which, in turn, seems to drive chromosome missegregation and aneuploidization.

Bub1 overexpression promotes spontaneous tumorigenesis

To address the fundamental question as to whether overexpression of Bub1 causally predisposes mice to spontaneous tumorigenesis, cohorts of wild-type, *Bub1*^{T85}, and *Bub1*^{T264} mice were aged to 12–16 mo and screened for tumors (Fig. 6 A). Overt tumors were collected and characterized by routine histopathology. Importantly, both transgenic strains had marked increases in tumor incidence compared with wild-type littermates (Fig. 6, A and B). Specifically, *Bub1*^{T85} and *Bub1*^{T264} mice had a total tumor incidence of 62 and 71%, respectively compared with 27% of wild-type mice, a difference that is highly statistically significant. The tumor spectrum of *Bub1* transgenic mice was broad and included lymphomas, lipomas, sarcomas, and liver and skin tumors (Fig. 6, C and D). *Bub1* transgenic mice also developed lung adenomas, but the incidence of these tumors was similar to control mice. A substantial proportion of *Bub1*

A

Genotype	Wild-type	Bub1^{T85}	Bub1^{T264}
Mice in study	26	29	24
Mice with tumors	7	18	17
Average Age (days)	497	510	474
Median Age (days)	503	522	490

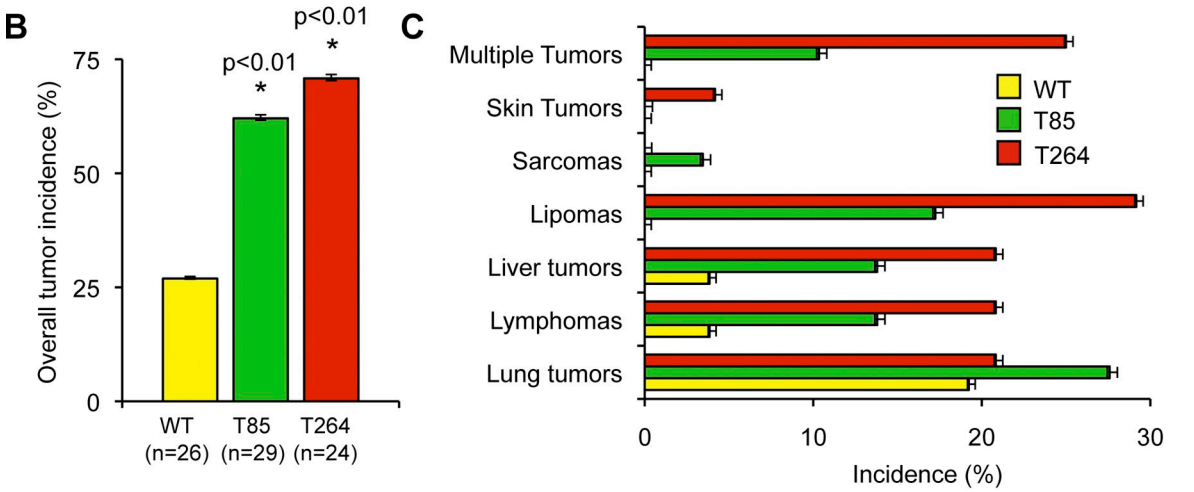

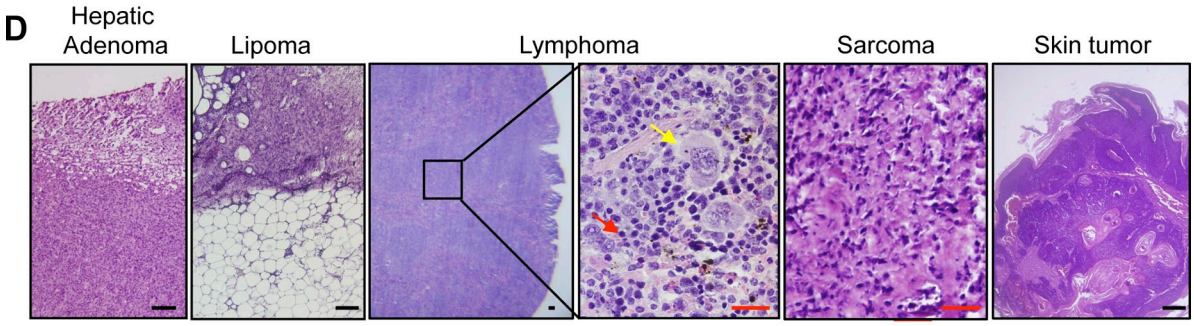

E

Mouse genotype	Tissue	Percent of cells with indicated chromosome 4 copies						Percent of cells with indicated chromosome 7 copies					
		1	2	3	4	5	6	1	2	3	4	5	6
WT	Normal liver 1	0	76	2	22	0	0	0	77	3	20	0	0
WT	Normal liver 2	1	79	0	20	0	0	0	80	1	19	0	0
T264	Liver tumor 1	1	40	29	28	0	2	1	35	10	44	7	3
T264	Liver tumor 2	3	78	4	14	1	0	3	76	7	13	0	1
WT	Normal spleen 1	2	98	0	0	0	0	2	98	0	0	0	0
WT	Normal spleen 2	0	100	0	0	0	0	2	98	0	0	0	0
WT	Normal spleen 3	1	99	0	0	0	0	2	98	0	0	0	0
T264	Splenic lymphoma 1	11	84	4	1	0	0	10	88	2	0	0	0
T264	Splenic lymphoma 2	10	89	1	0	0	0	5	95	0	0	0	0
T264	Splenic lymphoma 3	4	88	7	1	0	0	5	94	1	0	0	0
T264	Splenic lymphoma 4	8	88	4	0	0	0	10	90	0	0	0	0

Figure 6. **Bub1 overexpression promotes spontaneous tumorigenesis.** (A) Mouse cohort information. Mice were sacrificed between 12 and 16 mo: the average age of the sacrificed animals is indicated per genotype. (B) Spontaneous tumor incidence of mice of the indicated genotypes. *, $P < 0.01$ vs. wild-type mice using Fisher's exact test. Error bars indicate 95% confidence interval. (C) Tumor spectrum of mice of the indicated genotypes. Error bars indicate 95% confidence interval. (D) Histological analysis of selected spontaneous tumors from transgenic mice. Black bar, 100 µm. Red bar, 25 µm. Yellow arrow, neoplastic cell; red arrow, normal cell. (E) Interphase FISH for chromosomes 4 and 7 on single cell suspensions of tumors from Bub1 transgenic mice. Normal tissues from age-matched wild-type mice were used as controls.

transgenic mice were simultaneously affected with more than one tumor type (Fig. 6 C), whereas wild-type mice only had a single type of tumor. To assess aneuploidy in *Bub1* transgenic tumors, we performed interphase FISH on single cell suspensions of lymphomas and liver tumors using probes to chromosomes 4 and 7 (Baker et al., 2009). Both splenic lymphomas and hepatocellular carcinomas from *Bub1* transgenic animals harbored significant amounts of aneuploid cells compared with age-matched wild-type tissue controls (Fig. 6 E), which is consistent with the idea that Bub1 overexpression drives tumorigenesis through aneuploidization. Together, these results firmly establish that *Bub1* overexpression can drive tumorigenesis in various types of tissues/cell types, and that the resulting tumors are aneuploid.

Bub1 overexpression in mice accelerates Eμ-Myc–induced lymphomagenesis

Gene expression profiling studies indicate that Bub1 is frequently targeted for up-regulation in diffuse large B cell lymphomas (Alizadeh et al., 2000; Basso et al., 2005). To validate this observation and to explore whether *Bub1* might be overexpressed in other B cell malignancies as well, we quantitated *Bub1* transcript levels in a panel of different human primary B cell lymphomas and leukemias, including chronic lymphocytic leukemia (CLL), diffuse large B cell lymphoma (DLBCL), follicular lymphoma (FL), mantle cell lymphoma (MCL), marginal zone lymphoma (MZL), and Burkitt's lymphoma (BL). As a control, we used human peripheral B cells from normal donors. As shown in Fig. 7 A, *Bub1* mRNA was increased ($P < 0.05$) in all cases, except CLL. Particularly high Bub1 transcript levels were observed in the BLs. Importantly, this fold increase was not observed for two other cell cycle–regulated mitotic checkpoint genes, *Bub1B* and *Mad1* (Fig. S5 A). To extend these observations, we analyzed Bub1 protein levels in the BL cell lines Ramos and Raji by Western blotting. Samples were normalized for pSer10-H3 to rule out differences in proliferative index. Compared with the FL-derived cell line DOHH2, Raji showed highly elevated Bub1 levels, whereas in Ramos the increase was more modest (Fig. 7 B). Importantly, corresponding increases in pH2A and pCenp-A were observed in Raji and Ramos (Fig. 7 B). These data are consistent with the notion that increased Bub1 activity can promote increased Aurora B activity.

Because of the high levels of Bub1 transcript in BLs, a lymphoma characterized by overexpression of the c-*MYC* proto-oncogene, we sought to investigate whether Bub1 and c-Myc overexpression might cooperate to drive malignant transformation of B cells. To do so, we intercrossed Eμ-*Myc* transgenic (Harris et al., 1988) and *Bub1*^{T85} mice and established cohorts of Eμ-*Myc*;*Bub1*^{T85}, Eμ-*Myc* mice, and *Bub1*^{T85} transgenic mice and monitored them daily for development of ill heath and overt tumors. Eμ-*Myc* single-transgenic animals developed lymphoma beginning at 11 wk and had a median survival of 21 wk (Fig. 7 C). Strikingly, Eμ-*Myc*;*Bub1*^{T85} double-transgenic mice developed lymphoma much faster; fatal lymphomas developed as early as 7 wk and the median survival was only 13 wk. None of the *Bub1*^{T85} transgenic mice developed obvious lymphoma or any other overt tumors over the 1-yr monitoring period. These data demonstrate that *Bub1* overexpression synergizes with c-Myc in B cell lymphomagenesis, and suggest that Bub1 plays a role in the pathogenesis of human B cell lymphoma. To determine the degree of aneuploidy in lymphomas from Eμ-*Myc* and Eμ-*Myc*;*Bub1*^{T85} mice, we performed interphase FISH on seven independent lymph node tumors per genotype. On average, mature tumors from Eμ-*Myc*;*Bub1*^{T85} mice were slightly, but significantly ($P < 0.05$), more aneuploid for chromosome 4 and chromosome 7 (Fig. 7 D and Fig. S5 B).

Discussion

Bub1 is expressed at high levels in various types of human cancers, but whether and how Bub1 overexpression can cause neoplastic transformation has remained unknown. Using a transgenic approach in mice, we provide evidence that Bub1 has oncogenic properties in several mouse tissues. Furthermore, we show that Bub1 is consistently overexpressed in human Burkitt's lymphomas and that transgenic Bub1 dramatically decreases tumor latency in a mouse model for this lymphoid malignancy. Our studies suggest that Bub1 overexpression drives neoplastic growth at least in part by promoting chromosome missegregation. We propose that Bub1 overexpression results in aberrant chromosome segregation due to hyperactivation of Aurora B. Four lines of evidence support this novel mechanism. First, Cenp-A, a centromere-associated protein that is targeted by Aurora B kinase in prophase (Zeitlin et al., 2001), and Knl1, a key component of the KMN network, were phosphorylated at a significantly higher rate in *Bub1* transgenic cells than in controls. Phosphorylation at serine 10 of histone H3, another known target of Aurora B (Adams et al., 2001; Giet and Glover, 2001), occurred at seemingly normal rates in *Bub1* transgenic cells (unpublished data). However, this is not the first example where deregulation of Aurora B differentially affects phosphorylation of its targets. For example, Aurora B down-regulation due to haspin kinase depletion similarly affected only a limited number of Aurora B substrates (Wang et al., 2010). The observation that not all substrates are equally affected by Bub1-dependent Aurora B hyperactivation is also consistent with the notion that the activation status of the Aurora B complex may control substrate specificity (Musacchio, 2010).

Second, the most common chromosome segregation error in Bub1-overexpressing cells is chromosome lagging in anaphase (Agarwal et al., 1997), a defect that cannot be detected by the mitotic checkpoint and that does not result in mitotic delay. Lagging chromosomes occur due to the merotelic attachments of chromosomes to the mitotic spindle, which are thought to arise frequently in normal cells (Cimini et al., 2003). Aurora B functions in the correction of merotelic kinetochore attachments (Andrews et al., 2004; Kline-Smith et al., 2004), and its hyperactivation provides a plausible explanation for the high incidence of lagging chromosomes in Bub1-overexpressing cells. Aurora B is thought to correct merotelic attachments by regulating the microtubule-depolymerizing activity of MCAK and the microtubule-capturing activity of Ndc80/Hec1 (Cheeseman et al., 2006; Knowlton et al., 2006). In addition to lagging chromosomes, we observed misaligned chromosomes in cells

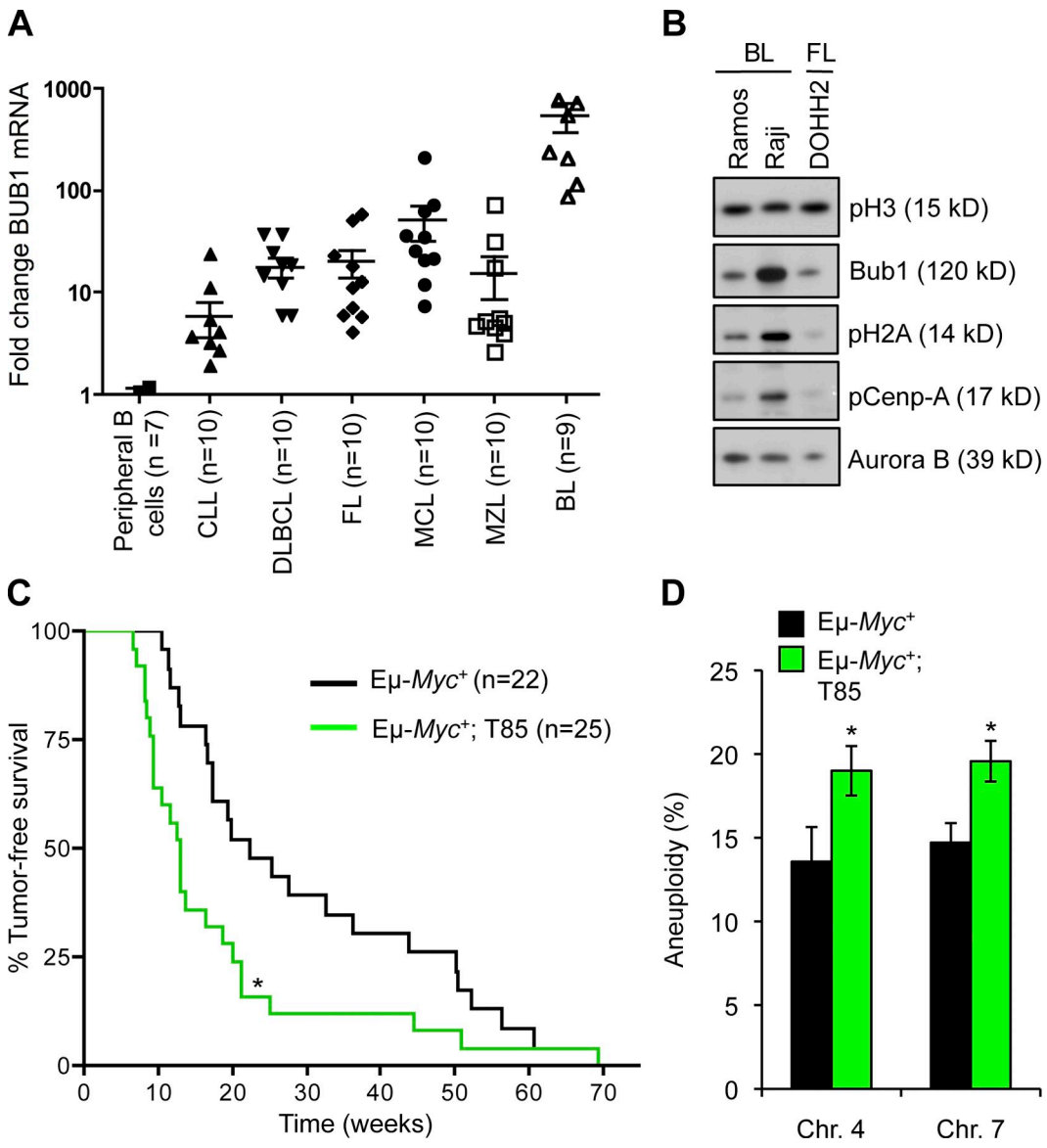

Figure 7. **Bub1 overexpression accelerates Myc-mediated lymphomagenesis.** (A) Human *Bub1* gene transcript was measured from a panel of 59 primary human tumors and normal peripheral B cells using qRT-PCR and normalized to TBP. The difference between lymphomas and normal peripheral B cells was statistically significant ($P < 0.05$) for all groups, except chronic lymphocytic leukemia. (B) Protein extracts from the indicated lymphoma derived cell lines were immunoblotted for Bub1, Aurora B, pCenp-A, pT121-H2A, and pS10-H3. (C) Survival curves for Eμ-*Myc* and Eμ-*Myc/Bub1*^{T85} mice. *, $P < 0.05$ vs. Eμ-*Myc* mice (log-rank test). (D) Quantification of chromosome 4 and 7 copies in EμMyc and Eμ-*Myc/Bub1*^{T85} B cell lymphoma cells. *, $P < 0.05$ (unpaired *t* test) FISH signals of 100 cells were per lymphoma. Seven lymphomas were analyzed per genotype. Error bars represent SEM.

with higher levels of overexpression (*Bub1*^{T264}). Interestingly, Aurora B has been shown to phosphorylate spatially distinct targets to differentially regulate the kinetochore–microtubule interface (Welburn et al., 2010). It is therefore tempting to speculate that a broader spectrum of Aurora B targets is deregulated in *Bub1*^{T264} cells than in *Bub1*^{T85} cells, thereby perhaps explaining why *Bub1*^{T264} cells have more diverse chromosome segregation errors. Given that modification of other CPC members has also been reported to affect Aurora B activity (Bishop and Schumacher, 2002; Bolton et al., 2002; Honda et al., 2003; Sessa et al., 2005; Jelluma et al., 2008) and various Aurora B subcomplexes (Gassmann et al., 2004), there could exist many different conformations of Aurora B–containing complexes, each with slightly different substrate specificity determined by the status of associated cofactors.

Third, inhibition of Aurora B activity, either pharmacologically with low amounts of ZM447439 or via BubR1 overexpression, largely corrected chromosome segregation errors caused by Bub1 overexpression. Although ZM447439 is a pan Aurora kinase inhibitor, at low concentrations, it preferentially targets Aurora B. Consistent with increased fidelity of chromosome segregation in *Bub1* transgenic cells that express high levels of BubR1 we find that these cells show significantly decreased aneuploidy rates. We note that, in contrast to *Bub1*, *BubR1* overexpression in and of itself does not cause chromosome missegregation (unpublished data).

Fourth, we show that a subset of Aurora B is in a complex with Bub1 during mitosis and that the abundance of this complex is considerably increased in *Bub1* transgenic cells. This raises

the possibility that Bub1 may affect Aurora B activity directly or indirectly by modulating the regulatory properties of CPC components. One potential mechanism for how Bub1 might alter Aurora B activity involves INCENP phosphorylation. *Xenopus* Bub1 has been shown to phosphorylate INCENP in vitro (Boyarchuk et al., 2007) and phosphorylation of INCENP at the C-terminal TSS motif has been linked to increased Aurora B kinase activity (Bishop and Schumacher, 2002; Honda et al., 2003). Unfortunately, we were unable to directly test this model experimentally because the residue(s) of INCENP that are modified by Bub1 are currently unknown.

Consistent with the idea that Bub1 might exert its oncogenic effect by targeting Aurora B for deregulation is the observation that sustained expression of Aurora B in cultured mouse mammary gland epithelial cells causes aneuploidy and promotes tumor development in a xenograft model (Nguyen et al., 2009). It will be important to expand these studies into the oncogenic potential of Aurora B, particularly because chromosome lagging due to merotelic attachments is a common trait of human cancer cells (Cimini, 2008; Kwon et al., 2008). Given that Aurora B activation is highly complex and involves multiple mechanisms, it is conceivable that defects in a wide variety of mitotic proteins cause Aurora B hyperactivation.

Recent evidence has demonstrated that Bub1 insufficiency leads to tumor development (Jeganathan et al., 2007; Baker et al., 2009). This, together with the transgenic study reported here, reveals that optimal Bub1 expression is critical for preventing neoplastic growth. Insufficiency and overexpression of Bub1 both result in whole chromosomal instability and near-diploid aneuploidies, although apparently through different mechanisms. Where Bub1 hypomorphism results in weakened checkpoint activity (Jeganathan et al., 2007), Bub1 overexpression does not seem to impair the checkpoint. This is surprising given that Bub1 has been proposed to contribute to checkpoint signaling via two mechanisms. First, Bub1 associates with kinetochores and this association is required for the kinetochore localization of core mitotic checkpoint proteins that produce the anaphase wait signal, including BubR1, Mad1, Mad2, and Cenp-E (Sharp-Baker and Chen, 2001; Morrow et al., 2005; Jeganathan et al., 2007; Perera et al., 2007). Second, Bub1 is thought to regulate checkpoint activity through inhibitory phosphorylation of the APC/C cofactor Cdc20 (Tang et al., 2004a). Earlier transgenic models overexpressing Mad2 or Hec1 presented evidence of mitotic checkpoint hyperactivation (Sotillo et al., 2007; Diaz-Rodríguez et al., 2008), but this mechanism of deregulating chromosome segregation does not seem to apply to Bub1 overexpression. Thus, high Bub1 levels activate an oncogenic mechanism that is unique among currently available transgenic mouse models. Furthermore, these findings illustrate that it is difficult to predict how overexpressed mitotic checkpoint genes perturb the chromosome segregation process, and underscores the importance of investigating the exact consequences of overexpression of each checkpoint gene.

In summary, our study demonstrates that Bub1 not only has tumor-suppressive but also oncogenic properties, which may explain why increased *Bub1* expression highly correlates with clinical prognosis in a variety of human cancer types (Glinsky, 2005; Glinsky et al., 2005). We provide a novel mechanism by which high Bub1 promotes aneuploidization. Given that losses and gains of whole chromosomes can drive tumorigenesis in certain genetic contexts (Baker et al., 2009; Holland and Cleveland, 2009; Baker and van Deursen, 2010; Schvartzman et al., 2010), it is reasonable to implicate Bub1-mediated hyperactivation of Aurora B in cellular transformation.

Materials and methods

Generation of Bub1 transgenic mice

Bub1 transgenic mice were generated according to previously described methods (van Ree et al., 2010, 2011). *Bub1* transgenic mice were maintained on a mixed 129SV/E × C57BL/6 genetic background. Eμ-*Myc* mice were bred with *Bub1*^{T85} mice to generate cohorts consisting of Eμ-*Myc*, and Eμ-*Myc*;*Bub1*^{T85} double-transgenic mice. Mice were housed in a pathogen-free barrier environment. Mouse protocols were reviewed and approved by the Mayo Clinic institutional animal care and use committee. Mice in tumor susceptibility studies were monitored daily. Moribund mice were killed and major organs screened for overt tumors. Tumors were processed for histopathology by standard procedures. Prism software was used for the generation of tumor-free survival curves and statistical analyses.

Generation and culture of MEFs

Bub1 transgenic MEFs were generated and cultured as described previously (Baker et al., 2004). MEFs were frozen at P2 or P3 and used for experimentation between P4 and P6. At least three independently generated MEF lines per genotype were used unless otherwise stated. Mitotic MEFs were prepared by two methods. Mitotic MEFs were collected after culturing asynchronous cells for 4 h in medium containing 100 ng/ml nocodazole (Sigma-Aldrich) and harvesting cells by shake-off. Alternatively, cells were synchronized in G_0 by serum starvation (0.1% FBS) for 12 h and released into 10% FBS containing DME. 0.5 μM taxol was then added 12 h after release and cells were harvested 18 h after release. Flag-tagged BubR1 was constitutively expressed using the Z/EG expression vector, similar to Bub1 (van Ree et al., 2010).

Cell culture, Western blot analysis, and immunoprecipitation

HeLa cells were cultured in DME supplemented with 10% FCS. Human cancer cell lines DOHH2, Ramos, and Raji were cultured in RPMI supplemented with 10% FCS. Western blot analysis was performed as described previously (van Ree et al., 2010). The following antibodies were used: rabbit anti-Bub1 (Jeganathan et al., 2007); 12CA5 or 16B12 (Santa Cruz Biotechnology, Inc. and Covance, respectively); pSer10-H3 (Millipore); β-actin (Sigma-Aldrich); Aurora B (BD); pT232-Aurora (Cell Signaling Technology); GFP (Takara Bio Inc.); pT121-H2A (Kawashima et al., 2010); H2A (Abcam); BubR1 (BD); Bub3 (J. van Deursen); and Mad2 (J. van Deursen). Immunoprecipitations for Aurora B and Bub1 were performed on mitotic cell extracts prepared in RIPA buffer (50 mM Tris, 150 mM NaCl, 0.1% SDS, 0.5% sodium deoxycholate, 1% NP-40, 1 mM EDTA, 1 mM EGTA, 20 mM β-glycerophosphate, 20 mM sodium fluoride, and 1 mM sodium vanadate, plus protease inhibitors). Antibodies for immunoprecipitation were Aurora B (BD) and Bub1 (Jeganathan et al., 2007). Mitotic HeLa cells were prepared from cells that were serum starved (0.1% FBS) for 12 h and released into 20% FBS containing DME. After 18 h, 0.5 μM taxol was added and cells were harvested 6 h later.

Indirect immunofluorescence and confocal microscopy

Indirect immunofluorescence was performed as described previously (Kasper et al., 1999). Cells were plated onto chamber slides and incubated for 24 h. Standard fixations for immunostainings were with 1% paraformaldehyde for 5 min at room temperature (RT). Primary antibodies, which were incubated overnight, were as follows: rabbit anti-Bub1 (Jeganathan et al., 2007); human anti-centromeric antibody (Antibodies Inc.); rabbit anti-Sgo1 (Abcam); rabbit anti-pCenp-A (Millipore); rabbit anti-pT121-H2A (Active Motif); rabbit anti-pKnl1 (Welburn et al., 2010); rabbit anti-Cdc20 (Santa Cruz Biotechnology, Inc.); rabbit anti–Mad2 (D. Cleveland, Ludwig Institute for Cancer Research, La Jolla, CA); mouse anti-BubR1 (BD); mouse anti-Aurora B (BD); rabbit anti-pThr232-Aurora (Cell Signaling Technology); and mouse anti-centrin2 (J. Salisbury, Mayo Clinic, Rochester, MN). A laser-scanning microscope (LSM 510 v3.2SP2; Carl Zeiss) with Axiovert 100M (Carl Zeiss) with a c-Apochromat 100x oil immersion objective was

used to analyze immunostained cells and to capture representative images. For quantification, we used ImageJ software (National Institutes of Health, Bethesda, MD). Confocal images were converted to 8-bit grayscale. Cell edges were traced using the freehand tool, and the mean pixel intensity within the marked area was calculated. The integrated density (in arbitrary units), defined as the mean pixel intensity multiplied by the area, was used to measure signal strength.

Quantitative RT-PCR

Total RNA was extracted using Trizol and cDNA transcription was performed using random hexamers and SuperScript III reverse transcription (Invitrogen). PCR reactions on cDNA from MEFs and mouse tissues were performed in triplicate with SYBR green PCR Master Mix using the ABI PRISM 7900 Sequence Detection System (Applied Biosystems). All experiments were performed on tissues from at least three animals in each group. TATA-binding protein (TBP) was used for normalization using ΔΔCt, except bone marrow, which was normalized to GAPDH. B and T cells were isolated from spleen using the MACS for $CD19^+$ cells or pan T cells (Miltenyi Biotec), respectively, after red blood cell lysis with ACK buffer (150 mM NH_4Cl, 10 mM $KHCO_3$, and 0.1 mM EDTA). PCR reactions were performed using the following reaction conditions: 95°C for 5 min, 40 cycles of 95°C for 30 s, 60°C for 30 s, and 72°C for 1 min, following with a dissociation stage to confirm a single PCR product. Primer sequences for qRT-PCR were as follows: TotalBub1for (p1): 5′-CATGAGCAGTGGGTTAGTGAAGAC-3′; TotalBub1rev (p2): 5′-TTCTCAGAAGCAGGAAGGTCCTTG-3′; EndoBub1for (p3): 5′-GTTTTTTCTCGTCATGGACAAC-3′; EndoBub1rev (p4): 5′-GTCATTACCCGTGTAGCTTTG-3′; TBPfor: 5′-GGCCTCTCAGAAGCATCACTA-3′; TBPrev: 5′-GCCAAGCCCTGAGCATAA-3′; GAPDHfor: 5′-TGCACCACACCAACTGCTTAGC-′3; GAPDHrev: 5′-TGGATGCAGGGATGATGTTC-3′. We detected endogenous Bub1 transcript with primers that anneals to the 5′ UTR. PCR reactions on cDNA isolated from primary human tumors and normal peripheral B cells were performed with Taqman probes (Bub1, 654643; TBP, 4332659; Mad1, 635627; Bub1B, 646627) using the ABI PRISM 7900 Sequence Detection System (Applied Biosystems).

Karyotype analysis and interphase FISH

Chromosome counts on metaphase spreads from P5 MEFs, splenocytes of 6-wk- and 5-mo-old mice, and hematopoietic cells in livers of 1-d-old mice were performed as described previously (Babu et al., 2003; Baker et al., 2004). In brief, cells were incubated with colcemid (0.5 µg/ml) for 4 to 6 h, swelled with 75 mM KCl, fixed (methanol/glacial acetic acid at 3:1), and stained with Giemsa. PMSCS was scored in cells where a majority of the sister chromosomes were no longer associated. Single cell suspensions of various tissues and tumors were hybridized with probes to chromosomes 4 and 7 for interphase FISH as described previously (Baker et al., 2009).

Live-cell imaging

For chromosome missegregation analysis, chromosome movements of mRFP-H2B–positive MEFs progressing through an unchallenged mitosis were followed at interframe intervals of 3 min and mitotic timing for the duration of prophase, prometaphase, metaphase, and anaphase was determined (Jeganathan et al., 2007; Dawlaty et al., 2008). In brief, MEFs were first transduced with a lentivirus encoding an mRFP-tagged H2B to allow visualization of chromosomes by fluorescence microscopy. Cells were seeded onto 35-mm glass-bottomed culture dishes and ∼24 h later were monitored using an Axio Observer Z1 system (Carl Zeiss) with: CO_2 Module S, TempModule S, Heating Unit XL S, Pln Apo 63x/1.4 oil DICIII objective, AxioCam MRm camera, and AxioVision 4.6 software. Nocodazole and taxol challenge assays and mitotic timing experiments were performed as described previously (Malureanu et al., 2009). At least three independent lines per genotype were used. To find a suitable concentration for partial inhibition of Aurora B activity, we followed progression of wild-type MEFs via live-cell imaging in the presence of various concentrations of ZM and determined the percentage of cells with mitotic arrest. We found mitotic arrest rates to drop to 15% at 2.5 nM ZM and therefore this concentration was selected for further experimentation.

Online supplemental material

Fig. S1 shows that levels of Bub1 and other mitotic regulators do not vary on 129 and C57BL/6 mouse genetic backgrounds. Fig. S2 shows that overexpression of Bub1 does not disrupt mitotic checkpoint signaling and mitotic timing. Fig. S3 shows that Aurora B localization and auto-phosphorylation is unaffected by Bub1 overexpression. Fig. S4 shows that treatment of *Bub1*^{T264} MEFs with 2.5 nM ZM447439 or co-overexpression of BubR1 does not diminish Bub1 kinase activity. Fig. S5 provides an analysis of *Bub1*, *Mad1*, and *BubR1* gene expression in human B cell malignancies and measurements of aneuploidy rates in Eμ-*Myc*$^+$ and Eμ-*Myc*$^+$;T85 transgenic mice. Online supplemental material is available at http://www.jcb.org/cgi/content/full/jcb.201012035/DC1.

We thank W. Zhou, and M. Li from the transgenic and gene knockout facility for generating *Bub1* transgenic mice; D. Norris and Dr. J. van Ree for help with mouse breeding and genotyping; the Mayo Clinic Cytogenetics shared resource for help with SKY/FISH analysis; and Drs. D. Baker, P. Galardy, L. Malureanu, J. van Ree, and R. Bram for helpful discussions and/or critical reading of the manuscript. We thank Drs. I. Cheeseman, Y. Watanabe, and J. Salisbury for sharing antibody and Drs. A. Novak and P. Galardy for lymphoma cell lines.

This work was supported by grants from the National Institutes of Health (CA126828 and CA96985; J.M. van Deursen) and a Leukemia and Lymphoma Society fellowship (R.M. Ricke).

Submitted: 7 December 2010
Accepted: 17 May 2011

References

Adams, R.R., H. Maiato, W.C. Earnshaw, and M. Carmena. 2001. Essential roles of *Drosophila* inner centromere protein (INCENP) and aurora B in histone H3 phosphorylation, metaphase chromosome alignment, kinetochore disjunction, and chromosome segregation. *J. Cell Biol.* 153:865–880. doi:10.1083/jcb.153.4.865

Agarwal, M.L., A. Agarwal, W.R. Taylor, Z.Q. Wang, E.F. Wagner, and G.R. Stark. 1997. Defective induction but normal activation and function of p53 in mouse cells lacking poly-ADP-ribose polymerase. *Oncogene*. 15:1035–1041. doi:10.1038/sj.onc.1201274

Alizadeh, A.A., M.B. Eisen, R.E. Davis, C. Ma, I.S. Lossos, A. Rosenwald, J.C. Boldrick, H. Sabet, T. Tran, X. Yu, et al. 2000. Distinct types of diffuse large B-cell lymphoma identified by gene expression profiling. *Nature*. 403:503–511. doi:10.1038/35000501

Andrews, P.D., Y. Ovechkina, N. Morrice, M. Wagenbach, K. Duncan, L. Wordeman, and J.R. Swedlow. 2004. Aurora B regulates MCAK at the mitotic centromere. *Dev. Cell*. 6:253–268. doi:10.1016/S1534-5807(04)00025-5

Babu, J.R., K.B. Jeganathan, D.J. Baker, X. Wu, N. Kang-Decker, and J.M. van Deursen. 2003. Rae1 is an essential mitotic checkpoint regulator that cooperates with Bub3 to prevent chromosome missegregation. *J. Cell Biol.* 160:341–353. doi:10.1083/jcb.200211048

Baker, D.J., and J.M. van Deursen. 2010. Chromosome missegregation causes colon cancer by APC loss of heterozygosity. *Cell Cycle*. 9:1711–1716. doi:10.4161/cc.9.9.11314

Baker, D.J., K.B. Jeganathan, J.D. Cameron, M. Thompson, S. Juneja, A. Kopecka, R. Kumar, R.B. Jenkins, P.C. de Groen, P. Roche, and J.M. van Deursen. 2004. BubR1 insufficiency causes early onset of aging-associated phenotypes and infertility in mice. *Nat. Genet.* 36:744–749. doi:10.1038/ng1382

Baker, D.J., F. Jin, K.B. Jeganathan, and J.M. van Deursen. 2009. Whole chromosome instability caused by Bub1 insufficiency drives tumorigenesis through tumor suppressor gene loss of heterozygosity. *Cancer Cell*. 16:475–486. doi:10.1016/j.ccr.2009.10.023

Basso, K., A.A. Margolin, G. Stolovitzky, U. Klein, R. Dalla-Favera, and A. Califano. 2005. Reverse engineering of regulatory networks in human B cells. *Nat. Genet.* 37:382–390. doi:10.1038/ng1532

Bishop, J.D., and J.M. Schumacher. 2002. Phosphorylation of the carboxyl terminus of inner centromere protein (INCENP) by the Aurora B Kinase stimulates Aurora B kinase activity. *J. Biol. Chem.* 277:27577–27580. doi:10.1074/jbc.C200307200

Bolton, M.A., W. Lan, S.E. Powers, M.L. McCleland, J. Kuang, and P.T. Stukenberg. 2002. Aurora B kinase exists in a complex with survivin and INCENP and its kinase activity is stimulated by survivin binding and phosphorylation. *Mol. Biol. Cell*. 13:3064–3077. doi:10.1091/mbc.E02-02-0092

Boyarchuk, Y., A. Salic, M. Dasso, and A. Arnaoutov. 2007. Bub1 is essential for assembly of the functional inner centromere. *J. Cell Biol.* 176:919–928. doi:10.1083/jcb.200609044

Cahill, D.P., C. Lengauer, J. Yu, G.J. Riggins, J.K. Willson, S.D. Markowitz, K.W. Kinzler, and B. Vogelstein. 1998. Mutations of mitotic checkpoint genes in human cancers. *Nature*. 392:300–303. doi:10.1038/32688

Cahill, D.P., L.T. da Costa, E.B. Carson-Walter, K.W. Kinzler, B. Vogelstein, and C. Lengauer. 1999. Characterization of MAD2B and other mitotic spindle checkpoint genes. *Genomics*. 58:181–187. doi:10.1006/geno.1999.5831

Carmena, M., S. Ruchaud, and W.C. Earnshaw. 2009. Making the Auroras glow: regulation of Aurora A and B kinase function by interacting proteins. *Curr. Opin. Cell Biol.* 21:796–805. doi:10.1016/j.ceb.2009.09.008

Cheeseman, I.M., J.S. Chappie, E.M. Wilson-Kubalek, and A. Desai. 2006. The conserved KMN network constitutes the core microtubule-binding site of the kinetochore. *Cell*. 127:983–997. doi:10.1016/j.cell.2006.09.039

Chung, E., and R.H. Chen. 2003. Phosphorylation of Cdc20 is required for its inhibition by the spindle checkpoint. *Nat. Cell Biol.* 5:748–753. doi:10.1038/ncb1022

Cimini, D. 2008. Merotelic kinetochore orientation, aneuploidy, and cancer. *Biochim. Biophys. Acta*. 1786:32–40.

Cimini, D., B. Moree, J.C. Canman, and E.D. Salmon. 2003. Merotelic kinetochore orientation occurs frequently during early mitosis in mammalian tissue cells and error correction is achieved by two different mechanisms. *J. Cell Sci.* 116:4213–4225. doi:10.1242/jcs.00716

Cimini, D., X. Wan, C.B. Hirel, and E.D. Salmon. 2006. Aurora kinase promotes turnover of kinetochore microtubules to reduce chromosome segregation errors. *Curr. Biol.* 16:1711–1718. doi:10.1016/j.cub.2006.07.022

Daum, J.R., J.D. Wren, J.J. Daniel, S. Sivakumar, J.N. McAvoy, T.A. Potapova, and G.J. Gorbsky. 2009. Ska3 is required for spindle checkpoint silencing and the maintenance of chromosome cohesion in mitosis. *Curr. Biol.* 19:1467–1472. doi:10.1016/j.cub.2009.07.017

Dawlaty, M.M., L. Malureanu, K.B. Jeganathan, E. Kao, C. Sustmann, S. Tahk, K. Shuai, R. Grosschedl, and J.M. van Deursen. 2008. Resolution of sister centromeres requires RanBP2-mediated SUMOylation of topoisomerase IIalpha. *Cell*. 133:103–115. doi:10.1016/j.cell.2008.01.045

DeLuca, K.F., S.M. Lens, and J.G. DeLuca. 2011. Temporal changes in Hec1 phosphorylation control kinetochore-microtubule attachment stability during mitosis. *J. Cell Sci.* 124:622–634. doi:10.1242/jcs.072629

Diaz-Rodríguez, E., R. Sotillo, J.M. Schvartzman, and R. Benezra. 2008. Hec1 overexpression hyperactivates the mitotic checkpoint and induces tumor formation in vivo. *Proc. Natl. Acad. Sci. USA*. 105:16719–16724. doi:10.1073/pnas.0803504105

Ditchfield, C., V.L. Johnson, A. Tighe, R. Ellston, C. Haworth, T. Johnson, A. Mortlock, N. Keen, and S.S. Taylor. 2003. Aurora B couples chromosome alignment with anaphase by targeting BubR1, Mad2, and Cenp-E to kinetochores. *J. Cell Biol.* 161:267–280. doi:10.1083/jcb.200208091

Ganem, N.J., S.A. Godinho, and D. Pellman. 2009. A mechanism linking extra centrosomes to chromosomal instability. *Nature*. 460:278–282. doi:10.1038/nature08136

Gassmann, R., A. Carvalho, A.J. Henzing, S. Ruchaud, D.F. Hudson, R. Honda, E.A. Nigg, D.L. Gerloff, and W.C. Earnshaw. 2004. Borealin: a novel chromosomal passenger required for stability of the bipolar mitotic spindle. *J. Cell Biol.* 166:179–191. doi:10.1083/jcb.200404001

Gemma, A., M. Seike, Y. Seike, K. Uematsu, S. Hibino, F. Kurimoto, A. Yoshimura, M. Shibuya, C.C. Harris, and S. Kudoh. 2000. Somatic mutation of the hBUB1 mitotic checkpoint gene in primary lung cancer. *Genes Chromosomes Cancer*. 29:213–218. doi:10.1002/1098-2264(2000)9999:9999<::AID-GCC1027>3.0.CO;2-G

Giet, R., and D.M. Glover. 2001. *Drosophila* aurora B kinase is required for histone H3 phosphorylation and condensin recruitment during chromosome condensation and to organize the central spindle during cytokinesis. *J. Cell Biol.* 152:669–682. doi:10.1083/jcb.152.4.669

Glinsky, G.V. 2005. Death-from-cancer signatures and stem cell contribution to metastatic cancer. *Cell Cycle*. 4:1171–1175. doi:10.4161/cc.4.9.2001

Glinsky, G.V., O. Berezovska, and A.B. Glinskii. 2005. Microarray analysis identifies a death-from-cancer signature predicting therapy failure in patients with multiple types of cancer. *J. Clin. Invest.* 115:1503–1521. doi:10.1172/JCI23412

Grabsch, H., S. Takeno, W.J. Parsons, N. Pomjanski, A. Boecking, H.E. Gabbert, and W. Mueller. 2003. Overexpression of the mitotic checkpoint genes BUB1, BUBR1, and BUB3 in gastric cancer—association with tumour cell proliferation. *J. Pathol.* 200:16–22. doi:10.1002/path.1324

Grabsch, H.I., J.M. Askham, E.E. Morrison, N. Pomjanski, K. Lickvers, W.J. Parsons, A. Boecking, H.E. Gabbert, and W. Mueller. 2004. Expression of BUB1 protein in gastric cancer correlates with the histological subtype, but not with DNA ploidy or microsatellite instability. *J. Pathol.* 202:208–214. doi:10.1002/path.1499

Harris, A.W., C.A. Pinkert, M. Crawford, W.Y. Langdon, R.L. Brinster, and J.M. Adams. 1988. The E mu-myc transgenic mouse. A model for high-incidence spontaneous lymphoma and leukemia of early B cells. *J. Exp. Med.* 167:353–371. doi:10.1084/jem.167.2.353

Hempen, P.M., H. Kurpad, E.S. Calhoun, S. Abraham, and S.E. Kern. 2003. A double missense variation of the BUB1 gene and a defective mitotic spindle checkpoint in the pancreatic cancer cell line Hs766T. *Hum. Mutat.* 21:445. doi:10.1002/humu.9120

Holland, A.J., and D.W. Cleveland. 2009. Boveri revisited: chromosomal instability, aneuploidy and tumorigenesis. *Nat. Rev. Mol. Cell Biol.* 10:478–487. doi:10.1038/nrm2718

Honda, R., R. Körner, and E.A. Nigg. 2003. Exploring the functional interactions between Aurora B, INCENP, and survivin in mitosis. *Mol. Biol. Cell*. 14:3325–3341. doi:10.1091/mbc.E02-11-0769

Jaffrey, R.G., S.C. Pritchard, C. Clark, G.I. Murray, J. Cassidy, K.M. Kerr, M.C. Nicolson, and H.L. McLeod. 2000. Genomic instability at the BUB1 locus in colorectal cancer, but not in non-small cell lung cancer. *Cancer Res.* 60:4349–4352.

Jeganathan, K., L. Malureanu, D.J. Baker, S.C. Abraham, and J.M. van Deursen. 2007. Bub1 mediates cell death in response to chromosome missegregation and acts to suppress spontaneous tumorigenesis. *J. Cell Biol.* 179:255–267. doi:10.1083/jcb.200706015

Jelluma, N., A.B. Brenkman, N.J. van den Broek, C.W. Cruijsen, M.H. van Osch, S.M. Lens, R.H. Medema, and G.J. Kops. 2008. Mps1 phosphorylates Borealin to control Aurora B activity and chromosome alignment. *Cell*. 132:233–246. doi:10.1016/j.cell.2007.11.046

Kang, J., I.M. Cheeseman, G. Kallstrom, S. Velmurugan, G. Barnes, and C.S. Chan. 2001. Functional cooperation of Dam1, Ipl1, and the inner centromere protein (INCENP)-related protein Sli15 during chromosome segregation. *J. Cell Biol.* 155:763–774. doi:10.1083/jcb.200105029

Kasper, L.H., P.K. Brindle, C.A. Schnabel, C.E. Pritchard, M.L. Cleary, and J.M. van Deursen. 1999. CREB binding protein interacts with nucleoporin-specific FG repeats that activate transcription and mediate NUP98-HOXA9 oncogenicity. *Mol. Cell. Biol.* 19:764–776.

Kawashima, S.A., Y. Yamagishi, T. Honda, K. Ishiguro, and Y. Watanabe. 2010. Phosphorylation of H2A by Bub1 prevents chromosomal instability through localizing shugoshin. *Science*. 327:172–177. doi:10.1126/science.1180189

Klebig, C., D. Korinth, and P. Meraldi. 2009. Bub1 regulates chromosome segregation in a kinetochore-independent manner. *J. Cell Biol.* 185:841–858. doi:10.1083/jcb.200902128

Kline-Smith, S.L., A. Khodjakov, P. Hergert, and C.E. Walczak. 2004. Depletion of centromeric MCAK leads to chromosome congression and segregation defects due to improper kinetochore attachments. *Mol. Biol. Cell*. 15:1146–1159. doi:10.1091/mbc.E03-08-0581

Knowlton, A.L., W. Lan, and P.T. Stukenberg. 2006. Aurora B is enriched at merotelic attachment sites, where it regulates MCAK. *Curr. Biol.* 16:1705–1710. doi:10.1016/j.cub.2006.07.057

Kulukian, A., J.S. Han, and D.W. Cleveland. 2009. Unattached kinetochores catalyze production of an anaphase inhibitor that requires a Mad2 template to prime Cdc20 for BubR1 binding. *Dev. Cell*. 16:105–117. doi:10.1016/j.devcel.2008.11.005

Kwon, M., S.A. Godinho, N.S. Chandhok, N.J. Ganem, A. Azioune, M. Thery, and D. Pellman. 2008. Mechanisms to suppress multipolar divisions in cancer cells with extra centrosomes. *Genes Dev.* 22:2189–2203. doi:10.1101/gad.1700908

Lampson, M.A., and T.M. Kapoor. 2005. The human mitotic checkpoint protein BubR1 regulates chromosome-spindle attachments. *Nat. Cell Biol.* 7:93–98. doi:10.1038/ncb1208

Luo, X., Z. Tang, J. Rizo, and H. Yu. 2002. The Mad2 spindle checkpoint protein undergoes similar major conformational changes upon binding to either Mad1 or Cdc20. *Mol. Cell*. 9:59–71. doi:10.1016/S1097-2765(01)00435-X

Malureanu, L.A., K.B. Jeganathan, M. Hamada, L. Wasilewski, J. Davenport, and J.M. van Deursen. 2009. BubR1 N terminus acts as a soluble inhibitor of cyclin B degradation by APC/C(Cdc20) in interphase. *Dev. Cell*. 16:118–131. doi:10.1016/j.devcel.2008.11.004

Meraldi, P., and P.K. Sorger. 2005. A dual role for Bub1 in the spindle checkpoint and chromosome congression. *EMBO J.* 24:1621–1633. doi:10.1038/sj.emboj.7600641

Morrow, C.J., A. Tighe, V.L. Johnson, M.I. Scott, C. Ditchfield, and S.S. Taylor. 2005. Bub1 and aurora B cooperate to maintain BubR1-mediated inhibition of APC/CCdc20. *J. Cell Sci.* 118:3639–3652. doi:10.1242/jcs.02487

Musacchio, A. 2010. Molecular biology. Surfing chromosomes (and Survivin). *Science*. 330:183–184. doi:10.1126/science.1197261

Nakagawa, T., T.M. Kollmeyer, B.W. Morlan, S.K. Anderson, E.J. Bergstralh, B.J. Davis, Y.W. Asmann, G.G. Klee, K.V. Ballman, and R.B. Jenkins. 2008. A tissue biomarker panel predicting systemic progression after PSA recurrence post-definitive prostate cancer therapy. *PLoS ONE*. 3:e2318. doi:10.1371/journal.pone.0002318

Nezi, L., and A. Musacchio. 2009. Sister chromatid tension and the spindle assembly checkpoint. *Curr. Opin. Cell Biol.* 21:785–795. doi:10.1016/j.ceb.2009.09.007

Nguyen, H.G., M. Makitalo, D. Yang, D. Chinnappan, C. St Hilaire, and K. Ravid. 2009. Deregulated Aurora-B induced tetraploidy promotes tumorigenesis. *FASEB J.* 23:2741–2748. doi:10.1096/fj.09-130963

Novak, A., C. Guo, W. Yang, A. Nagy, and C.G. Lobe. 2000. Z/EG, a double reporter mouse line that expresses enhanced green fluorescent protein upon Cre-mediated excision. *Genesis*. 28:147–155. doi:10.1002/1526-968X(200011/12)28:3/4<147::AID-GENE90>3.0.CO;2-G

O'Gorman, S., N.A. Dagenais, M. Qian, and Y. Marchuk. 1997. Protamine-Cre recombinase transgenes efficiently recombine target sequences in the male germ line of mice, but not in embryonic stem cells. *Proc. Natl. Acad. Sci. USA*. 94:14602–14607. doi:10.1073/pnas.94.26.14602

Perera, D., V. Tilston, J.A. Hopwood, M. Barchi, R.P. Boot-Handford, and S.S. Taylor. 2007. Bub1 maintains centromeric cohesion by activation of the spindle checkpoint. *Dev. Cell*. 13:566–579. doi:10.1016/j.devcel.2007.08.008

Peters, J.M. 2006. The anaphase promoting complex/cyclosome: a machine designed to destroy. *Nat. Rev. Mol. Cell Biol.* 7:644–656. doi:10.1038/nrm1988

Pouwels, J., A.M. Kukkonen, W. Lan, J.R. Daum, G.J. Gorbsky, T. Stukenberg, and M.J. Kallio. 2007. Shugoshin 1 plays a central role in kinetochore assembly and is required for kinetochore targeting of Plk1. *Cell Cycle*. 6:1579–1585. doi:10.4161/cc.6.13.4442

Ricke, R.M., J.H. van Ree, and J.M. van Deursen. 2008. Whole chromosome instability and cancer: a complex relationship. *Trends Genet.* 24:457–466. doi:10.1016/j.tig.2008.07.002

Roberts, B.T., K.A. Farr, and M.A. Hoyt. 1994. The *Saccharomyces cerevisiae* checkpoint gene BUB1 encodes a novel protein kinase. *Mol. Cell. Biol.* 14:8282–8291.

Sato, M., Y. Sekido, Y. Horio, M. Takahashi, H. Saito, J.D. Minna, K. Shimokata, and Y. Hasegawa. 2000. Infrequent mutation of the hBUB1 and hBUBR1 genes in human lung cancer. *Jpn. J. Cancer Res.* 91:504–509.

Schliekelman, M., D.O. Cowley, R. O'Quinn, T.G. Oliver, L. Lu, E.D. Salmon, and T. Van Dyke. 2009. Impaired Bub1 function in vivo compromises tension-dependent checkpoint function leading to aneuploidy and tumorigenesis. *Cancer Res.* 69:45–54. doi:10.1158/0008-5472.CAN-07-6330

Schvartzman, J.M., R. Sotillo, and R. Benezra. 2010. Mitotic chromosomal instability and cancer: mouse modelling of the human disease. *Nat. Rev. Cancer*. 10:102–115. doi:10.1038/nrc2781

Sessa, F., M. Mapelli, C. Ciferri, C. Tarricone, L.B. Areces, T.R. Schneider, P.T. Stukenberg, and A. Musacchio. 2005. Mechanism of Aurora B activation by INCENP and inhibition by hesperadin. *Mol. Cell*. 18:379–391. doi:10.1016/j.molcel.2005.03.031

Sharp-Baker, H., and R.H. Chen. 2001. Spindle checkpoint protein Bub1 is required for kinetochore localization of Mad1, Mad2, Bub3, and CENP-E, independently of its kinase activity. *J. Cell Biol.* 153:1239–1250. doi:10.1083/jcb.153.6.1239

Shichiri, M., K. Yoshinaga, H. Hisatomi, K. Sugihara, and Y. Hirata. 2002. Genetic and epigenetic inactivation of mitotic checkpoint genes hBUB1 and hBUBR1 and their relationship to survival. *Cancer Res.* 62:13–17.

Shigeishi, H., N. Oue, H. Kuniyasu, A. Wakikawa, H. Yokozaki, T. Ishikawa, and W. Yasui. 2001. Expression of Bub1 gene correlates with tumor proliferating activity in human gastric carcinomas. *Pathobiology*. 69:24–29. doi:10.1159/000048754

Silkworth, W.T., I.K. Nardi, L.M. Scholl, and D. Cimini. 2009. Multipolar spindle pole coalescence is a major source of kinetochore mis-attachment and chromosome mis-segregation in cancer cells. *PLoS ONE*. 4:e6564. doi:10.1371/journal.pone.0006564

Sironi, L., M. Mapelli, S. Knapp, A. De Antoni, K.T. Jeang, and A. Musacchio. 2002. Crystal structure of the tetrameric Mad1-Mad2 core complex: implications of a 'safety belt' binding mechanism for the spindle checkpoint. *EMBO J.* 21:2496–2506. doi:10.1093/emboj/21.10.2496

Sotillo, R., E. Hernando, E. Díaz-Rodríguez, J. Teruya-Feldstein, C. Cordón-Cardo, S.W. Lowe, and R. Benezra. 2007. Mad2 overexpression promotes aneuploidy and tumorigenesis in mice. *Cancer Cell*. 11:9–23. doi:10.1016/j.ccr.2006.10.019

Sotiriou, C., S.Y. Neo, L.M. McShane, E.L. Korn, P.M. Long, A. Jazaeri, P. Martiat, S.B. Fox, A.L. Harris, and E.T. Liu. 2003. Breast cancer classification and prognosis based on gene expression profiles from a population-based study. *Proc. Natl. Acad. Sci. USA*. 100:10393–10398. doi:10.1073/pnas.1732912100

Sudakin, V., G.K. Chan, and T.J. Yen. 2001. Checkpoint inhibition of the APC/C in HeLa cells is mediated by a complex of BUBR1, BUB3, CDC20, and MAD2. *J. Cell Biol.* 154:925–936. doi:10.1083/jcb.200102093

Tang, Z., H. Shu, D. Oncel, S. Chen, and H. Yu. 2004a. Phosphorylation of Cdc20 by Bub1 provides a catalytic mechanism for APC/C inhibition by the spindle checkpoint. *Mol. Cell*. 16:387–397. doi:10.1016/j.molcel.2004.09.031

Tang, Z., Y. Sun, S.E. Harley, H. Zou, and H. Yu. 2004b. Human Bub1 protects centromeric sister-chromatid cohesion through Shugoshin during mitosis. *Proc. Natl. Acad. Sci. USA*. 101:18012–18017. doi:10.1073/pnas.0408600102

Tang, Z., H. Shu, W. Qi, N.A. Mahmood, M.C. Mumby, and H. Yu. 2006. PP2A is required for centromeric localization of Sgo1 and proper chromosome segregation. *Dev. Cell*. 10:575–585. doi:10.1016/j.devcel.2006.03.010

Taylor, S.S., and F. McKeon. 1997. Kinetochore localization of murine Bub1 is required for normal mitotic timing and checkpoint response to spindle damage. *Cell*. 89:727–735. doi:10.1016/S0092-8674(00)80255-X

van Ree, J.H., K.B. Jeganathan, L. Malureanu, and J.M. van Deursen. 2010. Overexpression of the E2 ubiquitin-conjugating enzyme UbcH10 causes chromosome missegregation and tumor formation. *J. Cell Biol.* 188:83–100. doi:10.1083/jcb.200906147

van Ree, J., W. Zhou, M. Li, and J.M. van Deursen. 2011. Transgenesis in mouse embryonic stem cells. *Methods Mol. Biol.* 693:143–162. doi:10.1007/978-1-60761-974-1_9

van't Veer, L.J., H. Dai, M.J. van de Vijver, Y.D. He, A.A. Hart, M. Mao, H.L. Peterse, K. van der Kooy, M.J. Marton, A.T. Witteveen, et al. 2002. Gene expression profiling predicts clinical outcome of breast cancer. *Nature*. 415:530–536. doi:10.1038/415530a

Wang, F., J. Dai, J.R. Daum, E. Niedzialkowska, B. Banerjee, P.T. Stukenberg, G.J. Gorbsky, and J.M. Higgins. 2010. Histone H3 Thr-3 phosphorylation by Haspin positions Aurora B at centromeres in mitosis. *Science*. 330:231–235. doi:10.1126/science.1189435

Welburn, J.P., M. Vleugel, D. Liu, J.R. Yates III, M.A. Lampson, T. Fukagawa, and I.M. Cheeseman. 2010. Aurora B phosphorylates spatially distinct targets to differentially regulate the kinetochore-microtubule interface. *Mol. Cell*. 38:383–392. doi:10.1016/j.molcel.2010.02.034

Wood, K.W., R. Sakowicz, L.S. Goldstein, and D.W. Cleveland. 1997. CENP-E is a plus end-directed kinetochore motor required for metaphase chromosome alignment. *Cell*. 91:357–366. doi:10.1016/S0092-8674(00)80419-5

Yao, X., A. Abrieu, Y. Zheng, K.F. Sullivan, and D.W. Cleveland. 2000. CENP-E forms a link between attachment of spindle microtubules to kinetochores and the mitotic checkpoint. *Nat. Cell Biol.* 2:484–491. doi:10.1038/35019518

Zeitlin, S.G., R.D. Shelby, and K.F. Sullivan. 2001. CENP-A is phosphorylated by Aurora B kinase and plays an unexpected role in completion of cytokinesis. *J. Cell Biol.* 155:1147–1157. doi:10.1083/jcb.200108125